Received: 23 September 2017 | Revised: 3 December 2017 | Accepted: 13 December 2017
DOI: 10.1002/ardp.201700299

FULL PAPER

DPhG ARCH PHARM
Archiv der Pharmazie

# Design, synthesis, and molecular docking of novel indole scaffold-based VEGFR-2 inhibitors as targeted anticancer agents

Hanaa M. Roaiah[1] | Iman A. Y. Ghannam[1] | Islam H. Ali[1] | Ahmed M. El Kerdawy[2,3] | Mamdouh M. Ali[4] | Safinaz E-S. Abbas[2] | Sally S. El-Nakkady[1]

[1] National Research Centre, Pharmaceutical and Drug Industries Research Division, Chemistry of Natural and Microbial Products Department, Cairo, Egypt

[2] Faculty of Pharmacy, Department of Pharmaceutical Chemistry, Cairo University, Cairo, Egypt

[3] Molecular Modeling Unit, Faculty of Pharmacy, Cairo University, Cairo, Egypt

[4] National Research Centre, Genetic Engineering and Biotechnology Division, Department of Biochemistry, Cairo, Egypt

**Correspondence**
Dr. Iman A. Y. Ghannam, National Research Centre, Pharmaceutical and Drug Industries Research Division, Chemistry of Natural and Microbial Products Department, El-Bohouth Street, Dokki, Cairo 12622, Egypt.
Email: iman.youssef.ghannam@gmail.com

**Funding information**
National Research Centre – Cairo – Egypt, Grant number: P100220

## Abstract

A series of new indole derivatives **1**–**18** was synthesized and tested for their cytotoxic activity on a panel of 60 tumor cell lines. Additionally, molecular docking was carried out to study their binding pattern and binding affinity in the VEGFR-2 active site using sorafenib as a reference VEGFR-2 inhibitor. Based on the molecular docking results, compounds **5a**, **5b**, **6**, **7**, **14b**, **18b**, and **18c** were selected to be evaluated for their VEGFR-2 inhibitory activity. Compound **18b** exhibited a broad-spectrum antiproliferative activity on 47 cell lines, with GI % ranging from 31 to 82.5%. Moreover, compound **18b** was the most potent VEGFR-2 inhibitor with an $IC_{50}$ value of 0.07 μM, which is more potent than that of sorafenib (0.09 μM). A molecular docking study attributed the promising activity of this series to their hydrophobic interaction with the VEGFR-2 binding site hydrophobic side chains and their hydrogen bonding interaction with the key amino acids Glu885 and/or Asp1046.

KEYWORDS
anticancer agents, indole, molecular docking, VEGFR-2 inhibitors

## 1 | INTRODUCTION

Cancer remains one of the most life-threatening diseases worldwide.[1] Moreover, most of cancer patients suffer from serious adverse toxicities upon conventional chemotherapy treatment. Consequently, there is a necessity for designing new chemotherapeutic agents targeting cancer cells with minimum side effects associated with the normal cells collateral damage.[2,3] Angiogenesis, or formation of new blood vessels, has a central role in the cancer development.[4] The new blood vessels formation allows local tumors growth and feeds their growth in different sites, hence enables malignant cells to escape from their primary origin, to enter into circulation and enhance metastasis elsewhere.[5]

The vascular endothelial growth factor receptor-2 (VEGFR-2), one of the tyrosine kinase receptors, is considered as the most important transducer of VEGF-dependent angiogenesis. VEGFR-2 is highly up-regulated in several solid tumors and plays a critical role in the process of tumor angiogenesis, hence VEGFR-2 inhibition emerged as a prime approach for discovering new therapies for many human angiogenesis-dependent malignancies.[6]

Sunitinib (Sutent®) (**I**), an FDA approved oxindole multi-targeted kinase inhibitor, simultaneously blocks VEGFRs, platelet derived growth factor receptors (PDGFRs), and stem cell factor (c-kit) receptor

  

and is used for the treatment of gastrointestinal stromal tumor (GIST) and advanced renal cell carcinoma (RCC); it has VEGFR-2 inhibition with $IC_{50}$ value of 38 nM.[7–11] PubChem 47037197 (**II**), 2-aryl benzimidazole derivative, is also a multi-targeted kinase inhibitor. It inhibits epidermal growth factor receptor (EGFR) and VEGFRs[12,13] (Figure 1).

Among the wide range of tested compounds as potential anticancer agents, the indole derivatives have been reported to exhibit remarkable antitumor activities; as an example, compound **III** showed an $IC_{50}$ value of 5.7 nM against MCF-7 breast carcinoma cell line.[14] CJM 126 (**IV**), a 2-aryl benzothiazole derivative, shows also an *in vitro* anticancer activity against MCF-7 cancer cell line.[15] Additionally, some bicyclic systems, such as the chromone derivatives (**V**, **VI**), have been reported to possess anticancer activities against MCF-7 and A549 lung cancer cell lines with $IC_{50}$ values of 8.91, 2.23, 11.5, and 1.73 μM, respectively.[16]

Motivated by the VEGFR-2 inhibitory and anticancer activities of **I–VI**, it seemed of interest to design and synthesize the target compounds **1–18**. 2-Phenylindoles **2–5** (class A) are derived from PubChem 47037197 (**II**) and the 3-substituted-2-phenylindoles **6–9** (class B) from the lead compound **III**.

Indole thiazolinones **14a–e** (class C) are structural hybrids from the lead compounds **I**, **V**, while indole imidazolones **17a–d** and **18a–c** (class D) are structural hybrids from the lead compounds **I**, **VI** (Figure 2).

The designed modifications aimed to highlight the effect of lipophilicity, electronic nature and steric parameters of the newly synthesized indole derivatives on the VEGFR-2 inhibitory and anticancer activities.

Herein, we report the synthesis, anticancer activity of the newly synthesized compounds **1–18**. A docking study was also performed. Based on the scoring energy and binding mode, some compounds were selected to investigate their mechanism of action as VEGFR-2 inhibitors.

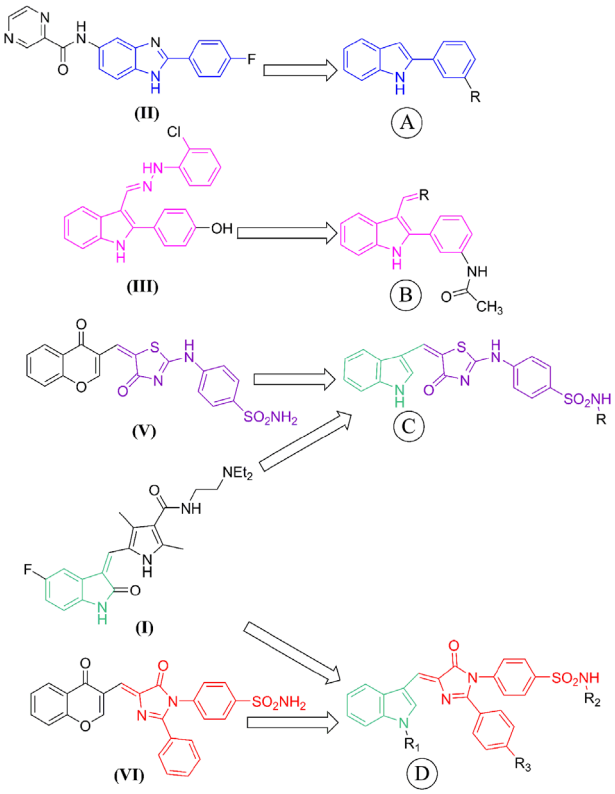


**FIGURE 2** Structural comparison of the target compounds classes (A–D) with sunitunib (**I**), PubChem 47037197 (**II**) and the anticancer compounds: indole derivative (**III**) and chromone derivatives (**V**, **VI**)

## 2 | RESULTS AND DISCUSSION

### 2.1 | Chemistry

In Scheme 1, 3-(1*H*-indol-2-yl)aniline **1** was synthesized via Fischer indole method.[17–19] Phenyl hydrazine was allowed to react with 3-aminoacetophenone to give the hydrazone which upon cyclization with polyphosphoric acid produced compound **1**.

Reaction of the amino functionality of **1** with the appropriate acid anhydride afforded compounds **2a**,**b**. IR spectra of both compounds revealed the appearance of two new carbonyl absorption bands at 1710–1713 $cm^{-1}$, whereas mass spectra disclosed molecular ion peaks at *m/z* 288 and 338, respectively. $^{1}$H-NMR spectrum of compound **2a** showed two new doublet signals at $\delta$ 7.41 and 7.90 ppm corresponding to the two protons of the pyrrole dione ring. $^{13}$C-NMR spectrum of **2b** revealed a signal at $\delta$ 167.6 ppm corresponding to the two carbonyl carbons.

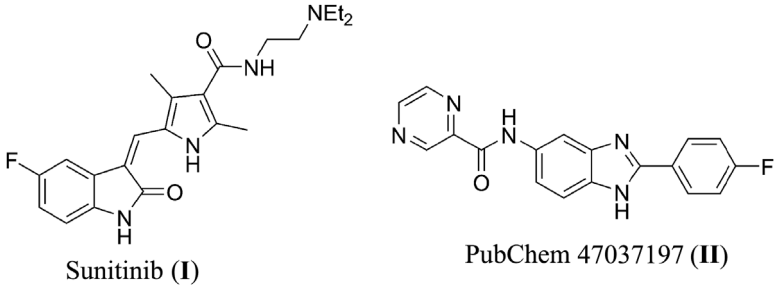


**FIGURE 1** Chemical structures of selected VEGFR-2 inhibitors: sunitunib (**I**) and PubChem 47037197 (**II**)

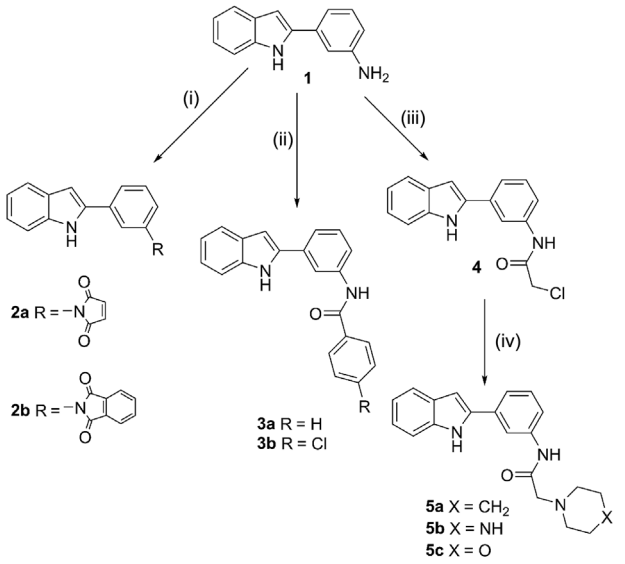


**SCHEME 1** Synthesis of target compounds **1–5**. Reagents and reaction conditions: (i) Acid anhydrides, glacial acetic acid, reflux, 2–3 h, yield: 40–45%. (ii) Acid chlorides, DMF, stirring, rt, 2 h, yield: 42–50%. (iii) Chloroacetyl chloride, DMF, stirring, rt, 1 h, yield: 52%. (iv) Secondary amines, DMF, $K_2CO_3$, stirring, rt, 1 h, yield: 55–60%

The *N*-substitued benzamide and 4-chlorobenzamide derivatives **3a**,**b** were obtained upon stirring **1** with the appropriate acid chloride in dimethylformamide at room temperature. IR spectra showed the appearance of a new amidic carbonyl absorption band in the region of 1650–1686 $cm^{-1}$. Furthermore, the mass spectrum of **3b** revealed a molecular ion peak at *m/z* 346 as a base peak. $^1$H-NMR spectra of compounds **3a**,**b** showed a new exchangeable singlet signal at $\delta$ 10.36 ppm corresponding to HN-C═O and an increase in the integration of aromatic protons was also noticed. $^{13}$C-NMR spectrum of **3b** revealed the appearance of a signal at $\delta$ 166.9 ppm attributed to the carbonyl carbon.

*N*-(3-(1*H*-Indol-2-yl)phenyl)-2-chloroacetamide **4** was formed via treating **1** with chloroacetyl chloride in dimethylformamide at room temperature. IR spectrum showed the appearance of a new amidic carbonyl band at 1677 $cm^{-1}$, whereas $^1$H-NMR spectrum revealed a new singlet signal at $\delta$ 4.29 ppm corresponding to $CH_2$-C═O protons in addition to a new exchangeable singlet signal at $\delta$ 10.39 ppm corresponding to HN-C═O. $^{13}$C-NMR spectrum showed the appearance of signals at $\delta$ 44.0 and 165.4 ppm corresponding to $CH_2$ and carbonyl carbons, respectively.

Reaction of **4** with the appropriate secondary amine in dimethylformamide at room temperature gave **5a–c**. $^1$H-NMR spectra disclosed the appearance of two multiplets at $\delta$ 1.43–1.61 and 2.45–2.47 ppm corresponding to piperidine protons, two multiplets at $\delta$ 2.46–2.50 and 2.60–2.68 ppm attributed to piperazine protons and two other multiplets at $\delta$ 2.47–2.48 and 3.66–3.69 ppm related to morpholine protons, respectively. Mass spectrum of **5b** illustrated a molecular ion peak at *m/z* 334. $^{13}$C-NMR spectrum of **5b** revealed the appearance of piperazine carbon signals at $\delta$ 46.0 and 53.3 ppm whereas compound **5c** showed signals at $\delta$ 53.8 and 66.7 ppm corresponding to morpholine carbons in addition to a signal at $\delta$ 62.6 ppm attributed to $CH_2$ carbon.

In Scheme 2, *N*-(3-(1*H*-indol-2-yl)phenyl)acetamide **6** was previously synthesized.[20] In our work, we synthesized it in a much simpler method; less reaction time and better product yield via refluxing of **1** in glacial acetic acid.

Vilsmeir Haack formylation reaction catalyzed by phosphorous oxychloride and *N*,*N*-dimethylformamide[21,22] was used to formylate compound **6** giving *N*-(3-(3-formyl-1*H*-indol-2-yl)phenyl)acetamide **7**.

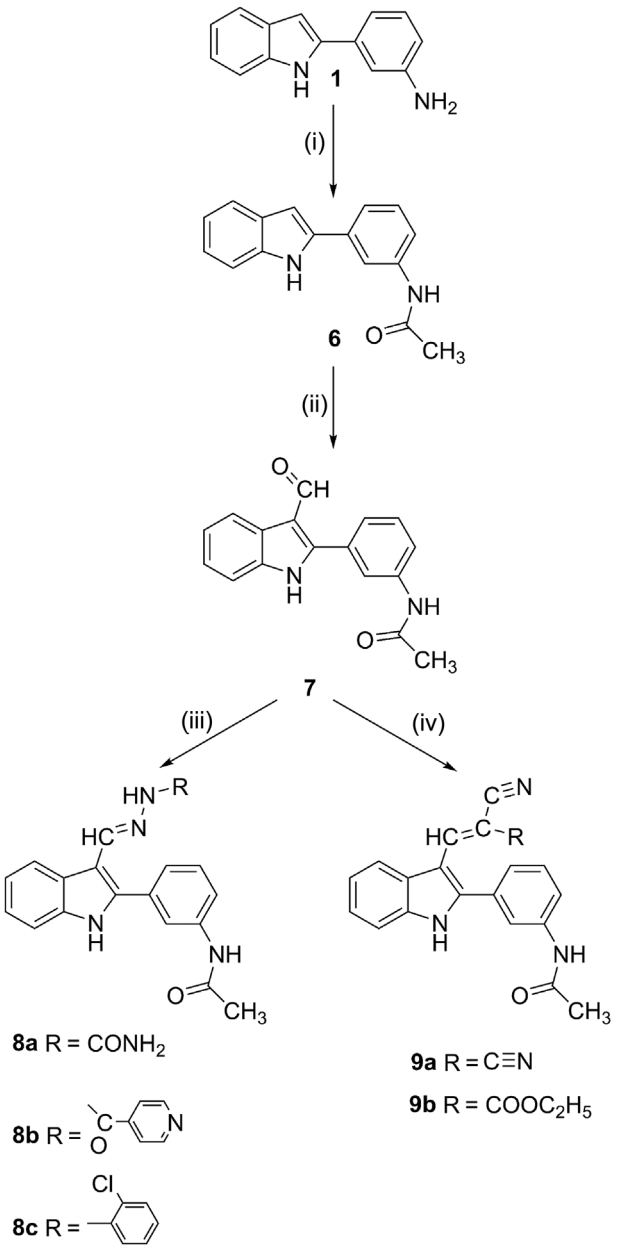


**SCHEME 2** Synthesis of target compounds **6–9**. Reagents and reaction conditions: (i) Glacial acetic acid, reflux, 3 h, yield: 64%. (ii) $POCl_3$, DMF, 1.5 h, yield: 35%. (iii) Semicarbazide HCl, isonicotinic acid hydrazide *o*-chlorophenylhydrazine HCl, EtOH, acetic acid, reflux, 2 h, yield: 30–37%. (iv) Active methylenes, EtOH, TEA, reflux, 3 h, yield: 42–49%

IR spectrum exhibited the appearance of an absorption band at 1676 $cm^{-1}$ attributed to (C═O aldehydic) and mass spectrum revealed a molecular ion peak at *m/z* 278. $^1$H-NMR spectrum of **7** illustrated the appearance of the aldehydic proton (HC═O) at *δ* 10.00 ppm in addition to lack of a singlet at *δ* 6.73 ppm that corresponds to H-3 indole. $^{13}$C-NMR spectrum disclosed a signal at *δ* 186.0 ppm attributed to aldehydic carbon.

Refluxing the formyl derivative **7** with semicarbazide hydrochloride, isonicotinic acid hydrazide, and *o*-chlorophenylhydrazine hydrochloride in ethanol using a catalytic amount of glacial acetic acid gave compounds **8a–c**, respectively. $^1$H-NMR spectra revealed the appearance of an azomethine (HC═N) as a singlet signal in the region *δ* 8.2–8.8 ppm in addition to lack of the aldehydic proton singlet signal *δ* 10.00 ppm. An extra exchangeable singlet signal at *δ* 9.55–11.76 ppm had also appeared corresponding to (N-NH). $^{13}$C-NMR spectrum of **8a** revealed the absence of the aldehydic carbonyl carbon signal at *δ* 186.0 ppm.

Reaction of **7** with active methylene derivatives as malononitrile or ethyl cyanoacetate was performed in refluxing ethanol in presence of triethylamine to produce compounds **9a**,**b**. IR spectra showed the absence of the carbonyl absorption bands of the aldehydic group, and showed the appearance of an absorption band of the cyano group in the region of 2214–2219 $cm^{-1}$ and the ester absorption band at 1683 $cm^{-1}$ for **9b**. $^1$H-NMR spectrum of **9b** demonstrated a triplet-quartet pattern of the ethyl protons at *δ* 1.27–1.29 and 4.22–4.29 ppm, respectively, and a singlet at *δ* 7.90 ppm related to the methine proton (CH═C). Mass spectra denoted the appearance of their molecular ion peaks at *m/z* 326 and 373, respectively.

In Scheme 3, a series of intermediates **10a–e**, **11a–e**, and **13** was first synthesized to produce **14a–e**. *N*-Chloroacetyl sulfonamide intermediates **10a–e** were prepared as previously reported by stirring a mixture of the appropriate sulfonamide and chloroacetyl chloride in dimethylformamide,[23,24] the intermediate thiazolidinones **11a–e** were also prepared according to the reported procedures by reacting **10a–e** with ammonium thiocyanate and refluxing in absolute ethanol.[16] Additionally, 1*H*-indole-3-carbaldehyde **13** was prepared as reported via Vilsmeir Haack formylation of the commercially available 1*H*-indole **12** using phosphorous oxychloride ($POCl_3$) and dimethylformamide (DMF).[25–29]

The target indole thiazolinones **14a–e** were synthesized by the Knoevenagel condensation reaction where indole-3-carbaldehyde **13** was reacted with thiazolidinones **11a–e** in glacial acetic acid in presence of sodium acetate.[16,30] $^1$H-NMR spectra of **14a–e** lacked the singlet signal at *δ* 4.00 ppm corresponding to the two protons of thiazolinone ring and displayed the appearance of a new singlet signal of the methine proton (—CH═) which appeared as a singlet signal at *δ* 7.93 ppm for **14a** or included within a multiplet in the aromatic region at *δ* 7.87–8.52 ppm for **14b–e**. On the other hand, $^{13}$C-NMR spectrum of **14a** showed the disappearance of $CH_2$ carbon signal of thiazolidinone intermediate **11a** at *δ* 37.6 ppm and the appearance of a new methine carbon (—CH═C) signal at *δ* 152.8 ppm. Compound **14a** was previously synthesized[31]; however, its physical properties and spectral data are reported in the present study for the first time.

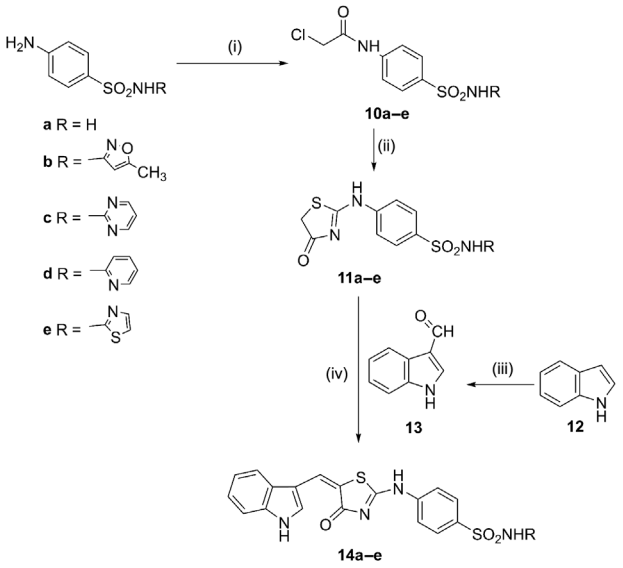


**SCHEME 3** Synthesis of target compounds **10–14**. Reagents and reaction conditions: (i) Chloroacetyl chloride, DMF, stirring, rt, 2–4 h yield: 60–80%. (ii) $NH_4SCN$, EtOH, reflux, 3–12 h, yield: 73–90%. (iii) $POCl_3$, DMF, 1.5 h, yield: 81%. (iv) Compound **13**, glacial acetic acid, sodium acetate, reflux, 5–21 h, yield: 40–60%

In Scheme 4, *N*-benzoyl/chlorobenzoylglycine intermediates **15a**, **b** were synthesized as reported by reaction of glycine with benzoyl/*p*-chlorobenzoyl chloride via stirring in sodium hydroxide solution.[32,33] Reaction of **13** with **15a**,**b** in acetic anhydride in the presence of anhydrous sodium acetate gave the indole oxazolone intermediates **16a**,**b**.[32,34] IR spectrum of the new compound **16b** illustrated the appearance of absorption bands at 1800 and 1685 $cm^{-1}$ corresponding to the oxazolone carbonyl and the amidic carbonyl groups, respectively, as well as the disappearance of NH indole absorption band. $^1$H-NMR spectrum of **16b** revealed two new singlets at *δ* 2.77 and 8.89 ppm corresponding to the $CH_3$ and methine CH═C protons, respectively.

In order to synthesize the target indole imidazolones **17a–d** and **18a–c**, indole oxazolones **16a**,**b** were reacted with the appropriate sulfonamide derivative in glacial acetic acid and in the presence of anhydrous sodium acetate. Upon monitoring the reaction rate by thin layer chromatography, it was noticed that compounds **17a–d** were synthesized within 1–2 h, while compounds **18a–c** were produced after 26–30 h. The difference in reaction time resulted in two different series of acetylated and deacetylated products **17a–d** and **18a–c**, respectively.

IR spectra of **17a–d** and **18a–c** revealed the appearance of imidazolone carbonyl absorption band at the region 1704–1715 $cm^{-1}$ and the disappearance of the oxazolone carbonyl absorption band at 1800 $cm^{-1}$. $^1$H-NMR spectra of **17a–d** showed the appearance of the singlet signal for O═C-$CH_3$ protons at *δ* 2.77 ppm, while this signal disappeared in the $^1$H-NMR spectra of **18a–c**. $^{13}$C-NMR spectra of **17a–d** confirmed that the acetyl group was retained due to the presence of two signals of acetyl carbons (N-CO-$CH_3$ and N-CO-$CH_3$) at *δ* 24.4 and 169.0 ppm, respectively.

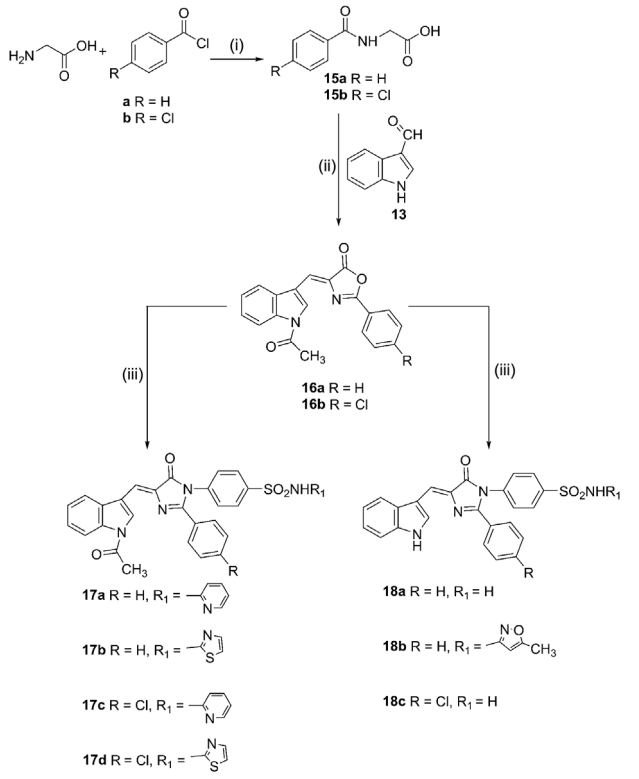


**SCHEME 4** Synthesis of target compounds **15**–**18**. Reagents and reaction conditions: (i) NaOH (10%), DMF, stirring, rt, 2 h, yield: 90–95%. (ii) Compound **13**, acetic anhydride, sodium acetate, reflux, 4 h, yield: 35–46%. (iii) Appropriate sulfonamide, glacial acetic acid, sodium acetate, reflux, 1–30 h, yield: 30–60%

## 2.2 | Molecular docking and structure–activity relationship

In the present study, we used PDB ID: 4ASD[35] which has VEGFR-2 in the inactive conformation (DFG-out) co-crystallized with sorafenib as inhibitor.

Initially, the docking protocol was validated by docking of the co-crystalized ligand sorafenib in the VEGFR-2 active site. The re-docking validation step efficiently reproduced the experimental binding pattern of the co-crystallized ligand indicating that the adapted docking protocol is suitable for the current docking study. The suitability of the docking setup is demonstrated by the small RMSD of 0.470 Å between the docking pose obtained in the validation step and the co-crystalized ligand and the ability of the docking pose to reproduce all the key interactions with the active site hotspots (Glu885, Cys919, and Asp1046). The scoring energy of the synthesized compounds (**1**–**18**) ranged from −8.61 to −17.4 kcal/mol compared with sorafenib calculated as −15.19 kcal/mol (for more details, see the Supporting Information).

For compound **1**, the molecular docking study showed a unique predicted binding pattern involving the fitting of the 2-phenylindole moiety in the middle of the active site at the interface between the ATP binding site and the hydrophobic allosteric back pocket directing its aminophenyl moiety toward the hydrophobic back pocket. In addition, the indole ring interacts by its NH as hydrogen bond donor through hydrogen bonding with the side chain carboxylate of Glu885 of the αC helix (Figure 3).

For the 3′-amido derivatives **2a–b**, **3a–b**, **4**, **5a–c**, **6**, and **7**, the general binding pattern involves the accommodation of the 2-phenyl indole moiety in the vicinity of the hydrophobic side chains of Val848, Lys868, Leu889, Val916, and Phe1047 amino acids to be involved in a hydrophobic interaction with these hydrophobic side chains. Furthermore, the amido extension at 3′-position of the phenyl ring is involved in hydrogen bonding interactions by its NH and CO functional groups with side chain carboxylate of Glu885 of the αC helix and DFG motif Asp1046, respectively. The hydrophobic moiety at the end of this extension is accommodated in the hydrophobic allosteric back pocket and so is involved in a hydrophobic interaction that increases the compounds' binding affinity[36] (for more details, see the Supporting Information).

Figure 4 shows compound **5a** adapting this aforementioned binding pattern with its piperidyl moiety accommodated in the VEGFR-2 hydrophobic allosteric back pocket and its amido moiety is involved in hydrogen bonding interactions with side chain carboxylate of Glu885 of the αC helix and DFG motif Asp1046. This binding pattern is

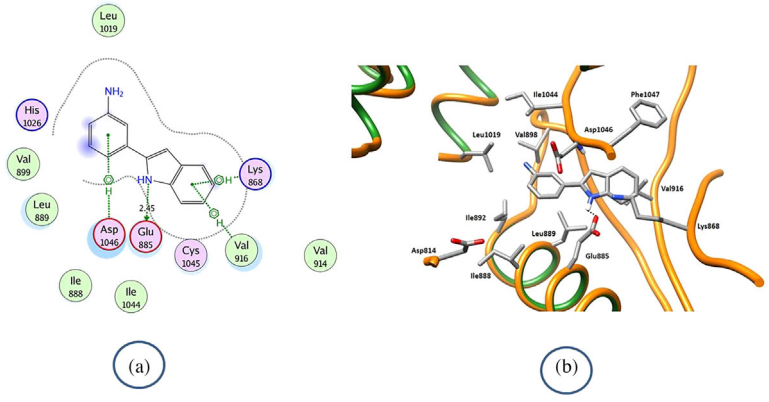


**FIGURE 3** 2D diagram (a) and 3D representation (b) of compound **1** showing its interaction with the VEGFR-2 receptor active site (distances in Å)

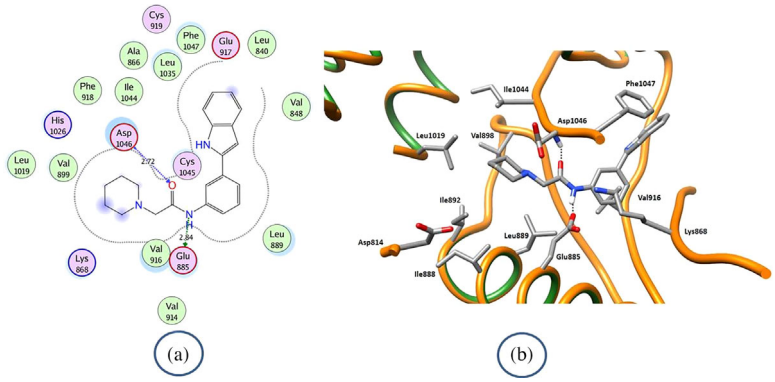


**FIGURE 4** 2D diagram (a) and 3D representation (b) of compound **5a** showing its interaction with the VEGFR-2 receptor active site (distances in Å)

responsible for the promising VEGFR-2 inhibitory activity of compound **5a** as indicated by its high *in vitro* VEGFR-2 level reducing effect in MCF-7 cell line of 79% and its $IC_{50}$ in VEGFR-2 inhibition assay of 1.14 µM.

For *N*-(3-(3-formyl-1*H*-indol-2-yl)phenyl)acetamide derivatives **8a–c**, **9a–b**, the general binding pattern involves the accommodation of the hydrophobic indole phenyl acetamide moiety in the hydrophobic back pocket of the active site lined with the hydrophobic side chains of amino acids Ile888, Leu889, Ile892, Val898, Val899, Leu1019 achieving hydrophobic interaction with these side chains. In addition, these compounds are involved in hydrogen bonding with the key amino acids Glu885 or/and Asp1046 through the substituent on the 3-position of the indole ring (Figure 5) (for more details, see the Supporting Information).

Sulfonamide derivatives **14a–e** adapted similar binding pattern to that of 3′-amido derivatives with their indolyl moiety accommodated in the hydrophobic vicinity of Val848, Lys868, Leu889, Val916, and Phe1047 side chains and involved in a hydrophobic interaction with them. In addition, the 2-amino-4-oxo-4,5-dihydrothiazolyl moiety accomplishes two hydrogen bond interactions through its ring N and NH at position 2 of the thiazolyl moiety with DFG motif Asp1046 and side chain carboxylate of Glu885, respectively. This binding pattern fits the benzene sulfonamide moiety in the hydrophobic allosteric back pocket of the VEGFR-2 binding site forming hydrophobic interaction through its phenyl moiety with the hydrophobic side chains of the amino acids lining this back pocket and hydrogen bond interaction through its sulfonamide moiety NH with the His1026 imidazole ring π electrons (for more details, see the Supporting Information).

Figure 6 shows that compound **14b** adapts this binding pattern rationalizing its promising VEGFR-2 inhibitory activity as indicated by its high *in vitro* VEGFR-2 level reducing effect in MCF-7 cell line of 61% and its $IC_{50}$ in VEGFR-2 inhibition assay of 1.87 µM.

Compounds **17a–d** and **18a–c** show a binding pattern which is consistent with that of these series of compounds with their indolyl moiety involved in a hydrophobic interaction with the hydrophobic side chains of Val848, Lys868, Leu889, Val916, and Phe1047 amino acids. Phenyl substituents at positions 2 and 3 of the imidazolyl moiety are accommodated in the hydrophobic allosteric back pocket and are involved in a hydrophobic interaction which is responsible for the pronounced VEGFR-2 inhibitory activity of this series as reflected in their docking scores (Supporting Information Table S1) and the experimental results (see below).

Figure 7 shows compound **18b** adapting this binding pattern which not only achieves the previously mentioned hydrophobic

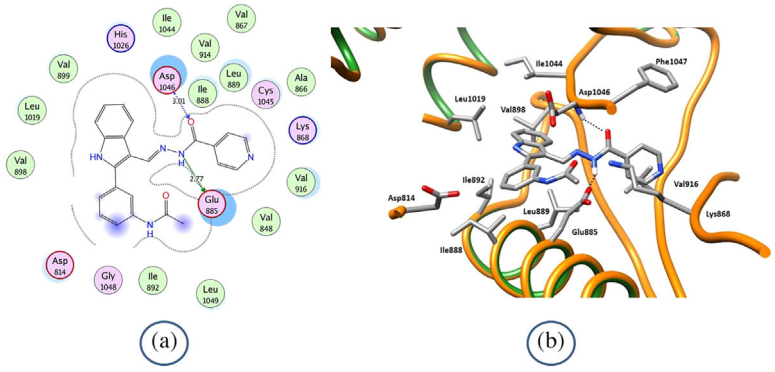


**FIGURE 5** 2D diagram (a) and 3D representation (b) of compound **8b** showing its interaction with the VEGFR-2receptor active site (distances in Å)

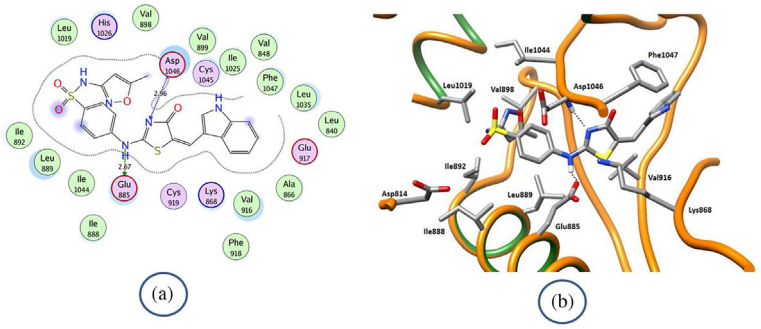


**FIGURE 6** 2D diagram (a) and 3D representation (b) of compound **14b** showing its interaction with the VEGFR-2 receptor active site (distances in Å)

interactions but also it forms hydrogen bonding interaction through its carbonyl oxygen at position 5 of the imidazolyl moiety with Lys868. These interactions ensure that compound **18b** possesses potential VEGFR-2 inhibitory activity as indicated by its promising $IC_{50}$ in VEGFR-2 inhibition assay of 0.07 µM and this is reflected in its docking score of −15.08 kcal/mol which is comparable to that of sorafenib (−15.19 kcal/mol).

In summary, the promising VEGFR-2 inhibitory activity of the newly synthesized compounds can be attributed to their hydrophobic interactions with the hydrophobic side chains of Val848, Lys868, Leu889, Val916, and Phe1047 amino acids and the hydrophobic allosteric back pocket of the active site lined with the hydrophobic side chains of amino acids Ile888, Leu889, Ile892, Val898, Val899, Leu1019. Besides, the ability of most of them to accomplish hydrogen bonding interactions with the active site key amino acids Glu885 and/or Asp1046.

## 2.3 | Biological studies

### 2.3.1 | *In vitro* antiproliferative activity

Twenty-three of the newly synthesized compounds were selected and tested for their *in vitro* antiproliferative activity by the National Cancer Institute (NCI), Bethesda, Maryland, USA,[37] under the Developmental Therapeutic Program (DTP).[38–42]

The selected compounds were evaluated at a concentration of 10 µM on a panel of 60 tumor cell lines representing melanoma, leukemia and lung, brain, colon, kidney, ovary, prostate, and breast cancers. A protocol of 48 h drug exposure and sulforhodamine B (SRB) protein assay was used to determine the cell viability and growth.

The antiproliferative activity was presented by the NCI as percent growth of the treated cells, and is presented in Table 1 as growth inhibition percentage (GI %) achieved by the tested compounds. The tested compounds exhibited diverse antiproliferative activities.

Compound **18b** (Table 1) exhibited antiproliferative activity against 47 cancer cell lines with GI % ranging from 31 to 82.5%. It showed potent growth inhibitory effects with GI % from 62 to 82.5% against leukemia (CCRF-CEM, HL-60(TB), MOLT-4, RPMI-8226 and SR), non-small cell lung (A549/ATTC and NCI-H460), colon (COLO 205, HCT-116, HCT-15, HT29 and KM12), CNS (U251, melanoma LOX IM VI, M 14 and MDA-MB-435), ovarian (OVCAR-8), renal (786-0 and UO-31), prostate (PC-3), and breast (MCF7 and T-47D) cell lines.

Regarding sensitivity to individual cell lines, it was noticed that the newly synthesized compounds show selectivity to nearly all leukemia cells, non-small cell lung (HOP-92), renal (A498 and UO-31), and breast (MDA-MB-231/ATTC) cell lines.

### 2.3.2 | *In vitro* determination of VEGFR-2 level for selected compounds in MCF-7 cell line

Recent studies showed the up-regulation of VEGFR-2 in MCF-7 cell line.[43,44] Based on the docking study results represented in the

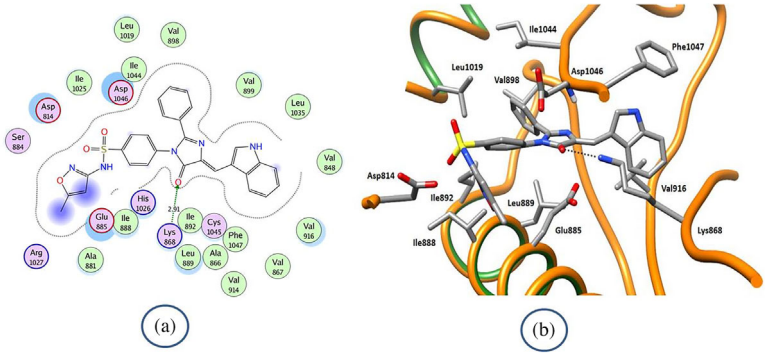


**FIGURE 7** 2D diagram (a) and 3D representation (b) of compound **18b** showing its interaction with the VEGFR-2 receptor active site (distances in Å)

**TABLE 1** Growth inhibition % (GI %) of the selected compounds *in vitro* against a panel of tumor cell lines at 10 μM

| | Compound ID | | | | | | | | | | | | |
|---|---|---|---|---|---|---|---|---|---|---|---|---|---|
| **Subpanel** | **3b** | **5a** | **5c** | **7** | **9a** | **9b** | **14c** | **14e** | **17a** | **17c** | **17d** | **18a** | **18b** |
| Leukemia | | | | | | | | | | | | | |
| CCRF-CEM | 41 | –[a] | – | – | – | – | – | – | 44 | 35 | 52 | – | 78 |
| HL-60(TB) | 32 | – | 31 | – | 33 | – | – | – | – | – | – | – | 73.5 |
| K-562 | 60 | 85 | – | – | – | – | – | – | – | 32 | 40 | – | – |
| MOLT-4 | 62 | 41 | – | – | – | – | – | – | – | 40 | 49 | – | 82.5 |
| PRMI-8226 | 40 | – | – | – | – | – | – | – | 58 | 39 | 38 | – | 76 |
| SR | 47.5 | 45 | – | – | – | – | – | – | – | 31 | 39 | – | 80.5 |
| Non-small cell lung cancer | | | | | | | | | | | | | |
| A549/ATTC | – | – | – | – | – | – | – | – | – | – | – | – | 61 |
| EKVX | 35 | – | – | – | – | – | – | – | – | – | – | – | 50 |
| HOP-62 | – | – | – | – | – | – | – | – | – | – | – | – | 41 |
| HOP-92 | 50 | 39 | – | 35 | 31 | 30 | – | – | – | – | – | – | 44 |
| NCI-H226 | – | – | – | – | – | – | – | – | – | – | – | – | 39 |
| NCI-H23 | 32.5 | – | – | – | – | – | – | – | – | – | – | – | – |
| NCI-H322M | – | – | – | – | – | – | – | – | – | – | – | – | – |
| NCI-H460 | – | – | – | – | – | – | – | – | – | – | – | – | 81 |
| NCI-H522 | 42 | – | – | – | – | – | – | – | – | – | 40 | – | 50 |
| Colon cancer | | | | | | | | | | | | | |
| COLO 205 | – | – | – | – | – | – | – | – | – | – | – | – | 63 |
| HCC-2998 | – | – | – | – | – | – | – | – | – | – | – | – | 35 |
| HCT-116 | 52 | – | – | – | – | – | – | – | – | – | – | – | 70 |
| HCT-15 | 35 | 49 | – | – | – | – | – | – | – | – | – | – | 75 |
| HT29 | 33 | 74 | – | – | – | – | – | – | – | – | – | – | 80 |
| KM12 | – | 30 | – | – | – | – | – | – | – | – | 30 | – | 76 |
| SW-620 | – | – | – | – | – | – | – | – | – | – | – | – | 43 |
| CNS cancer | | | | | | | | | | | | | |
| SF-268 | – | – | – | – | – | – | – | – | – | – | – | – | 53 |
| SF-295 | – | – | – | – | – | – | – | – | – | – | – | – | 50 |
| SF-539 | – | – | – | – | – | – | – | – | – | – | – | – | 44.5 |
| SNB-19 | – | – | – | – | – | – | – | – | – | – | 32 | – | 45 |
| SNB-75 | 34 | – | – | – | – | – | – | – | – | – | – | – | 45 |
| U251 | | 33 | – | – | – | – | – | – | – | – | 44 | – | 65 |
| Melanoma | | | | | | | | | | | | | |
| LOX IMVI | 32.5 | – | – | – | – | – | – | – | – | – | – | – | 66 |
| MALME-3M | – | – | – | – | – | – | – | – | – | – | – | – | – |
| M14 | – | – | – | – | – | – | – | – | – | – | – | – | 62 |
| MDA-MB-435 | – | – | – | – | 35.5 | – | – | – | – | – | – | – | 63 |
| SK-MEL-2 | – | – | – | – | – | – | – | – | – | – | – | – | – |
| SK-MEL-28 | – | – | – | – | – | – | – | – | – | – | – | – | 35 |
| SK-MEL-5 | – | – | – | – | – | – | – | – | – | – | – | – | N.D. |
| UACC-257 | – | – | – | – | – | – | – | – | – | – | – | – | – |
| UACC-62 | 39 | – | – | – | – | – | – | – | – | – | – | – | 35 |

(Continues)

**TABLE 1** (Continued)

| | Compound ID | | | | | | | | | | | | |
|---|---|---|---|---|---|---|---|---|---|---|---|---|---|
| **Subpanel** | **3b** | **5a** | **5c** | **7** | **9a** | **9b** | **14c** | **14e** | **17a** | **17c** | **17d** | **18a** | **18b** |
| Ovarian cancer | | | | | | | | | | | | | |
| IGROV1 | – | – | – | – | – | – | – | – | – | – | – | – | 40 |
| OVCAR-3 | – | – | – | – | – | – | – | – | – | – | – | – | 51 |
| OVCAR-4 | 38 | – | – | – | – | – | – | – | – | – | – | – | 53 |
| OVCAR-5 | – | – | – | – | – | – | – | – | – | – | – | – | – |
| OVCAR-8 | – | – | – | – | – | – | – | – | 38 | – | 34 | – | 62 |
| NCI/ADR-RES | – | – | – | – | – | – | – | – | – | – | – | – | – |
| SK-OV-3 | – | – | – | – | – | – | – | – | – | – | – | – | – |
| Renal cancer | | | | | | | | | | | | | |
| 786-0 | – | – | – | – | – | – | – | – | – | – | – | – | 67.5 |
| A498 | 32 | 32 | – | – | – | – | – | – | 39 | – | – | 33 | 39 |
| RXF 393 | – | – | – | – | – | – | – | – | – | – | – | – | 51 |
| SN 12C | – | – | – | – | – | – | – | – | – | – | – | – | 41.5 |
| TK-10 | – | – | – | – | – | – | – | – | – | – | – | – | – |
| UO-31 | 38 | – | – | – | 37 | 33 | 31 | 33 | – | – | – | – | 70 |
| Prostate cancer | | | | | | | | | | | | | |
| PC-3 | 47 | – | – | – | – | – | – | – | – | – | – | – | 73.5 |
| DU-145 | – | – | – | – | – | – | – | – | – | – | – | – | 46 |
| Breast cancer | | | | | | | | | | | | | |
| MCF7 | 32 | – | – | – | – | – | – | – | – | – | 50 | – | 75 |
| MDA-MB-231/ATTC | 50 | 54 | – | – | 30 | 30 | – | – | – | – | – | – | 50 |
| HS 578T | – | – | – | – | – | – | – | – | – | – | – | – | 43.5 |
| BT-549 | – | – | – | – | – | – | – | – | – | – | – | – | 50 |
| T-47D | 37.5 | – | – | – | 30 | – | – | – | – | – | 44 | – | 62 |
| MDA-MB-468 | 54 | – | – | – | 32.5 | – | – | – | – | – | – | – | 31 |

[a]Growth inhibition % produced by the compound is below 30%.

compounds scoring energy and binding mode in the VEGFR-2 active site, 10 of the newly synthesized compounds were selected for the evaluation of their effect on VEGFR-2 level in human breast cancer MCF-7 cell line. The effect of the tested compounds on VEGFR-2 as a marker for angiogenesis was determined as triplicate determinations (Table 2).

Compounds **5a**, **6**, **14b**, and **18c** showed potent inhibitory effect of the VEGFR-2 level in (MCF-7) cell line as compared to the untreated cancer cells with percentage inhibition values of 79, 68, 61, and 85%, respectively. While sorafenib, the reference compound used in this test, showed a percentage reduction value of 84%.

### 2.3.3 | *In vitro* VEGFR-2 kinase inhibitory assay

Based on their docking results in the VEGFR-2 active site and testing the effect on cellular VEGFR-2 level, seven compounds (**5a**, **5b**, **6**, **7**, **14b**, **18b**, and **18c**) were chosen for further evaluation of their VEGFR-2 inhibitory activity using the VEGFR-2 kinase inhibitory kit assay. $IC_{50}$ of the selected tested compounds are given in Table 3 and compared with sorafenib as a reference standard.

As seen in Table 3, the seven tested compounds displayed moderate to potent VEGFR-2 inhibitory activities. Compounds **5a** and **6** exhibited good potency with $IC_{50}$ values of 1.14 and 1.11 μM, respectively. Compound **18b** was the most potent showing an $IC_{50}$ value of 0.07 μM as compared to sorafenib $IC_{50}$ (0.09 μM).

## 3 | CONCLUSION

A series of indole based analogs **1–18** was synthesized. Most of the synthesized compounds were chosen by the NCI DTP in Bethesda (Rockville, MD) for testing their antiproliferative action on a panel of 60 cell lines and compound **18b** exhibited a broad antiproliferative activity on numerous cell lines. It was noticed that there was selectivity to nearly all leukemia cell lines, non-small cell lung cancer (HOP-92), renal cancer (A498 and UO-31), and breast cancer (MDA-MB-231/ATTC).

**TABLE 2** *In vitro* determination of VEGFR-2 level for selected compounds in MCF-7 cell line

| Compound ID | $IC_{50}$ MCF-7 (μM)[a] | VEGFR-2 level (ng/mL)[b] | VEGFR-2 inhibition (%)[c] |
|---|---|---|---|
| DMSO | – | 1978.76 ± 236.00 | – |
| **3b** | 34.7 | 1790.48 ± 188.00 | 9.5 |
| **5a** | 13 | 410.10 ± 45.13 | 79 |
| **5b** | 53.3 | 1800.11 ± 195.00 | 9 |
| **6** | 16 | 632.85 ± 77.11 | 68 |
| **8b** | 90.6 | 1970.00 ± 220.47 | 0.4 |
| **14a** | 54.3 | 1860.40 ± 190.34 | 6 |
| **14b** | 17.3 | 766.81 ± 80.16 | 61 |
| **14d** | 87.4 | 1970.80 ± 223.76 | 0.4 |
| **14e** | 83.2 | 1965.80 ± 211.70 | 0.65 |
| **18c** | 11.4 | 291.88 ± 30.00 | 85 |
| Sorafenib | 6.12 | 320.60 ± 36.50 | 84 |

[a]The concentration of each compound required to produce 50% inhibition of cell growth.
[b]Data were recorded as mean of three independent experiments.
[c]Percentage inhibition as compared with control untreated cells.

Compounds **5a**, **6**, **14b**, and **18c** showed potent reducing effect on VEGFR-2 level in human breast cancer cell line (MCF-7) as compared to the untreated cancer cells with percentage inhibition values of 79, 68, 61, and 85%, respectively. The synthesized compounds were docked into sorafenib VEGFR-2 active site and based on the docking study results, seven compounds (**5a**, **5b**, **6**, **7**, **14b**, **18b**, and **18c**) were selected for further VEGFR-2 inhibitory study. Compound **18b** proved to be more potent than sorafenib with $IC_{50}$ values of 0.07 and 0.09 μM, respectively. Molecular docking study attributed the remarkable activity of this series to their hydrophobic interactions with the hydrophobic side chains of Val848, Lys868, Leu889, Val916, and Phe1047 amino acids and the hydrophobic allosteric back pocket of the active site lined with the hydrophobic side chains of amino acids Ile888, Leu889, Ile892, Val898, Val899, Leu1019. Besides, the ability of most of them to accomplish hydrogen bonding interactions with the active site key amino acids Glu885 and/or Asp1046.

**TABLE 3** $IC_{50}$ (μM) values of selected compounds on VEGFR-2

| Compound ID | VEGFR-2 $IC_{50}$ (μM)[a] |
|---|---|
| **5a** | 1.14 |
| **5b** | 3.18 |
| **6** | 1.11 |
| **7** | 2.13 |
| **14b** | 1.87 |
| **18b** | 0.07 |
| **18c** | 1.61 |
| Sorafenib | 0.09 |

[a]The concentration recorded to produce 50% inhibition of VEGFR-2.

## 4 | EXPERIMENTAL

### 4.1 | Chemistry

#### 4.1.1 | General

All chemicals and solvents used were purchased from commercial suppliers. Thin layer chromatography (TLC) was performed on precoated silica gel 60 F245 aluminium sheets (Merck) and visualized using Vilber Lourmet ultraviolet lamp at λ = 254 nm. Melting points were recorded by open capillary tube method using an Electrothermal melting point apparatus and are uncorrected. Spectral data and elemental analysis were performed at the Central Services Unit – National Research Centre (NRC) and Microanalytical Units – Faculty of Science and Faculty of Pharmacy – Cairo University – Cairo – Egypt. Infra-red spectra were recorded using KBr pellets on a Jasco FT/IR 6100 spectrophotometer. $^{1}$H- and $^{13}$C-NMR spectra were performed at 400 (100) MHz recorded on a Bruker AVANCE III Nano Bay FT-NMR spectrophotometer using dimethylsulfoxide (DMSO-$d_6$) as a solvent. Chemical shifts (δ) are given in parts per million (ppm) relative to tetramethylsilane (TMS) as an internal standard. Coupling constants are reported in Hertz (Hz). Mass spectra were recorded on FINNIGAN MAT SSQ 7000 digital DEC 3000 and JEOL JMS-AX 500 mass spectrometers. Elemental analysis was performed on a Vario EL Elementar.

The InChI codes of the investigated compounds together with some biological activity data are provided as Supporting Information.

**3-(1*H*-Indol-2-yl)aniline (1)**[17–19]

It was reported to be synthesized by Fischer indole method. In our work, we reported its synthesis for the first time via polyphosphoric acid (PPA) as a cyclizing agent. Yield (90%); m.p. 133°C, (Lit. 136°C).[19]

#### 4.1.2 | General procedure for the synthesis of 2-(3-(1*H*-indol-2yl)phenyl)pyrroledione and isoindoline derivatives (2a,b)

3-(1*H*-indol-2-yl)aniline **1** (0.5 g, 2.4 mmol) and the appropriate acid anhydride (2.4 mmol) were refluxed in least amount of glacial acetic acid (5 mL) for 2–3 h. The solution was left to concentrate in air, water was added and the precipitate was collected, washed with water and crystallized from acetone for compound **2b** while compound **2a** was purified by column chromatography using ethyl acetate/petroleum ether (80:100) in a ratio of 3:2.

**1-(3-(1*H*-Indol-2-yl)phenyl)-1*H*-pyrrole-2,5-dione (2a)**

White crystals (yield 40%); m.p. 157–159°C; reaction time 2 h; IR (KBr) $cm^{-1}$: 3352 (NH), 1708 (C═O); $^{1}$H-NMR (DMSO-$d_6$) (δ, ppm): 6.93 (s, 1H, H-3 indole); 6.99–7.03 (m, 1H, Ar-H); 7.10–7.14 (m, 1H, Ar-H); 7.24–7.28 (m, 3H, Ar-H); 7.41 (d, 1H, CH pyrrole dione,

*J* = 8 Hz); 7.54–7.60 (m, 2H, Ar-H); 7.82–7.83 (m, 1H, Ar-H); 7.90 (d, 1H, CH pyrrole dione, *J* = 8 Hz); 11.60 (s, 1H, NH indole, $D_2O$ exchangeable); EIMS, *m/z*: 288 ($M^+$); Anal. calcd. for $C_{18}H_{12}N_2O_2$ (288.09): C, 74.99; H, 4.20; N, 9.72; O, 11.10. Found: C, 74.38; H, 3.98; N, 9.45; O, 11.22.

**2-(3-(1*H*-Indol-2-yl)phenyl)isoindoline-1,3-dione (2b)**

Green crystals (yield 45%); m.p. 95–97°C; reaction time 3 h; IR (KBr) $cm^{-1}$: 3368 (NH), 3054 (CH aromatic), 1713 (2C═O); $^1$H-NMR (DMSO-$d_6$) (*δ*, ppm): 6.73 (s, 1H, H-3 indole); 6.90–7.08 (m, 3H, Ar-H); 7.35–7.63 (m, 4H, Ar-H); 7.91–8.14 (m, 5H, Ar-H); 11.61 (s, 1H, NH indole, $D_2O$ exchangeable); $^{13}$C-NMR (DMSO-$d_6$) (*δ*, ppm): 99.9, 111.9, 116.0, 117.3, 120.4, 120.7, 121.0, 122.3, 123.0, 124.0, 124.5, 126.9, 129.8, 131.0, 132.0, 133.1, 135.3, 167.5; EIMS, *m/z*: 338 ($M^+$); Anal. calcd. for $C_{22}H_{14}N_2O_2$ (338.11): C, 78.09; H, 4.17; N, 8.28; O, 9.46. Found: C, 77.81; H, 4.64; N, 8.31; O, 9.36.

### 4.1.3 | General procedure for the synthesis of *N*-(3-(1*H*-indol-2-yl)phenyl)benzamide/4-chlorobenzamide derivatives (3a,b)

To a well stirred solution of 3-(1*H*-indol-2-yl)aniline **1** (0.5 g, 2.4 mmol) in dry dimethylformamide (3 mL), the appropriate acid chloride (2.4 mmol) was dropwisely added with continuous stirring on cold for 2 h. The solution was poured onto ice/water, the formed precipitate was collected, washed with water and crystallized from ethanol for compound **3b** while compound **3a** was purified by column chromatography using ethyl acetate/petroleum ether (80:100) in a ratio of 3:2.

***N*-(3-(1*H*-Indol-2-yl)phenyl)benzamide (3a)**

Commercially available, CAS Registry Number: 1115499-93-8; whitish yellow crystals (yield 42%); m.p. 222–224°C; IR (KBr) $cm^{-1}$: 3429, 3394 (NH), 1650 (C═O amidic); $^1$H-NMR (DMSO-$d_6$) (*δ*, ppm): 6.8 (s, 1H, H-3 indole); 6.99–7.03 (m, 1H, Ar-H); 7.09–7.13 (m, 1H, Ar-H); 7.4–7.5 (m, 2H, Ar-H); 7.55–7.7 (m, 5H, Ar-H); 8–8.03 (m, 2H, Ar-H); 8.25–8.3 (m, 1H, Ar-H); 10.36 (s, 1H, NHCO, $D_2O$ exchangeable); 11.55 (s, 1H, NH indole, $D_2O$ exchangeable); Anal. calcd. for $C_{21}H_{16}N_2O$ (312.13): C, 80.75; H, 5.16; N, 8.97; O, 5.12. Found: C, 80.81; H, 5.64; N, 8.31; O, 5.36.

***N*-(3-(1*H*-Indol-2-yl)phenyl)-4-chlorobenzamide (3b)**

Green crystals (yield 50%); m.p. 172–174°C; IR (KBr) $cm^{-1}$: 3413 (NH), 1686 (C═O amidic); $^1$H-NMR (DMSO-$d_6$) (*δ*, ppm): 6.83 (s, 1H, H-3 indole); 7.01–7.02 (m, 1H, Ar-H); 7.09–7.13 (m, 1H, Ar-H); 7.41–7.48 (m, 2H, Ar-H); 7.57 (d, 2H, Ar-H, *J* = 8.4 Hz); 7.61–7.67 (m, 2H, Ar-H); 7.95 (d, 2H, Ar-H, *J* = 8.4 Hz); 8.05 (d, 1H, Ar-H, *J* = 8.4 Hz); 8.29 (s, 1H, Ar-H); 10.43 (s, 1H, NH-C═O, $D_2O$ exchangeable); 11.56 (s, 1H, NH indole, $D_2O$ exchangeable); $^{13}$C-NMR (DMSO-$d_6$) (*δ*, ppm): 99.2, 111.9, 118.0, 119.9, 120.4, 121.2, 122.1, 129.0, 129.2, 129.7, 130.1, 131.6, 133.2, 134.0, 137.7, 138.1, 138.3, 139.9, 166.9; EIMS, *m/z*: 348 ($M^+$+2), 346 ($M^+$); Anal. calcd. for $C_{21}H_{15}ClN_2O$ (346.09): C, 72.73; H, 4.36; N, 8.08; O, 4.61; Cl, 10.22. Found: C, 72.38; H, 3.98; N, 8.45; O, 4.22; Cl, 10.45.

### 4.1.4 | Synthesis of *N*-(3-(1*H*-indol-2-yl)phenyl)-2-chloroacetamide (4)

To a well stirred solution of 3-(1*H*-indol-2-yl)aniline **1** (0.5 g, 2.4 mmol) in dry dimethylformamide (5 mL), chloroacetyl chloride (0.3 mL, 2.4 mmol) was dropwisely added with continuous stirring on cold for 1 h. The solution was poured onto ice/water, the obtained precipitate was collected, washed with water and purified by column chromatography using ethyl acetate/petroleum ether (80:100) in a ratio of 3:2. Yield 52%; m.p. 209–211°C; IR (KBr) $cm^{-1}$: 3406, 3278 (NH indole, NH-C═O), 1677 (C═O amidic); $^1$H-NMR (DMSO-$d_6$) (*δ*, ppm): 4.29 (s, 2Hs, O═C-C$H_2$-Cl); 6.80 (s, 1H, H-3 indole); 6.95–7.13 (m, 2H, Ar-H); 7. 40–7.60 (m, 5H, Ar-H); 8.01–8.02 (m, 1H, Ar-H); 10.39 (s, 1H, NHC═O, $D_2O$ exchangeable); 11.53 (s, 1H, NH indole, $D_2O$ exchangeable); $^{13}$C-NMR (DMSO-$d_6$) (*δ*, ppm): 44.0, 99.3, 111.9, 116.8, 119.3, 119.9, 120.6, 121.2, 122.2, 129.0, 129.9, 133.4, 137.7, 138.0, 139.4, 165.3; Anal. calcd. for $C_{16}H_{13}ClN_2O$ (284.07): C, 67.49; H, 4.60; N, 9.84; O, 5.62; Cl, 12.45. Found: C, 67.79; H, 4.80; N, 10.14; O, 5.22; Cl, 12.25.

### 4.1.5 | General procedure for the synthesis of *N*-(3-(1*H*-indol-2-yl)phenyl)-2-(piperidine/piperazin/morpholine-1-yl)acetamide (5a–c)

To a well stirred solution of *N*-(3-(1*H*-indol-2-yl)phenyl)-2-chloroacetamide **4** (0.5 g, 1.8 mmol) in dry dimethylformamide (3 mL), the appropriate secondary amine (2 mmol) was added in the presence of (0.2 g, 2.2 mmol) anhydrous potassium carbonate with continuous stirring on cold for 1 h. The solution was poured onto ice/water to give a precipitate which was collected, washed with water and crystallized from acetone for compound **5a** and ethanol for compounds **5b** and **5c**.

***N*-(3-(1*H*-Indol-2-yl)phenyl)-2-(piperidin-1-yl)acetamide (5a)**

Green crystals (yield 55%); m.p. 112–114°C; IR (KBr) $cm^{-1}$: 3409, 3283 (NH), 1673 (C═O amidic); $^1$H-NMR (DMSO-$d_6$) (*δ*, ppm): 1.43–1.61 (m, 6H, piperidine H); 2.45–2.47 (m, 4H, piperidine H) 3.07 (s, 2H, C$H_2$); 6.83 (s, 1H, H-3 indole); 6.97–7.12 (m, 2H, Ar-H); 7.37–7.62 (m, 5H, Ar-H); 8.05–8.06 (m, 1H, Ar-H); 9.68 (s, 1H, NHCO, $D_2O$ exchangeable); 11.48 (s, 1H, NH indole, $D_2O$ exchangeable); Anal. calcd. for $C_{21}H_{23}N_3O$ (333.18): C, 75.65; H, 6.95; N, 12.60; O, 4.80. Found: C, 75.38; H, 6.38; N, 12.85; O, 4.22.

***N*-(3-(1*H*-Indol-2-yl)phenyl)-2-(piperazin-1-yl)acetamide (5b)**

Green crystals (yield 60%); m.p. 125–127°C; IR (KBr) $cm^{-1}$: 3318 (NH), 1703 (C═O amidic); $^1$H-NMR (DMSO-$d_6$) (*δ*, ppm): 2.46–2.50 (m, 4H, piprazine H); 2.60–2.68 (m, 4H, piprazine H); 3.30 (s, 2H, C$H_2$); 3.36 (s, 1H, NH piprazine, $D_2O$ exchangeable); 6.83 (s, 1H, H-3 indole); 6.97–7.20 (m, 2H, Ar-H); 7.40–7.61 (m, 5Hs, Ar-H); 8.07–8.09 (m, 1H, Ar-H); 9.75 (s, 1H, NHCO, $D_2O$ exchangeable); 11.50 (s, 1H, NH indole, $D_2O$ exchangeable); $^{13}$C-NMR (DMSO-$d_6$) (*δ*, ppm): 46.0, 53.2, 62.3,

99.3, 111.9, 116.9, 119.2, 119.9, 120.6, 120.8, 122.1, 129.0, 129.8, 133.3, 137.6, 138.0, 139.56, 169.0 EIMS, *m/z*: 334 ($M^+$); Anal. calcd. for $C_{20}H_{22}N_4O$ (334.41): C, 71.83; H, 6.63; N, 16.75; O, 4.78. Found: C, 71.61; H, 6.94; N, 16.31; O, 4.96.

#### *N*-(3-(1*H*-Indol-2-yl)phenyl)-2-morpholinoacetamide (5c)

Green crystals (yield 57%); m.p. 193–195°C; IR (KBr) $cm^{-1}$: 3412, 3281 (NH), 1669 (C═O amidic); $^1$H-NMR (DMSO-$d_6$) (δ, ppm): 2.47–2.48 (m, 4H, morpholine H); 3.14 (s, 2H, C$\underline{H}_2$-C═O); 3.66–3.69 (m, 4H, morpholine H); 6.82 (s, 1H, H-3 indole); 6.99–7.20 (m, 2H, Ar-H); 7.40–7.59 (m, 5H, Ar-H); 8.07–8.08 (m, 1H, Ar-H); 9.77 (s, 1H, N$\underline{H}$CO, $D_2O$ exchangeable); 11.48 (s, 1H, NH indole, $D_2O$ exchangeable); $^{13}$C-NMR (DMSO-$d_6$) (δ, ppm): 53.7, 62.6, 66.6, 99.3, 111.9, 116.9, 119.3, 119.9, 120.6, 120.8, 122.1, 129.0, 129.7, 133.2, 137.6, 138.0, 139.5, 168.8; Anal. calcd. for $C_{20}H_{21}N_3O_2$ (335.40): C, 71.62; H, 6.31; N, 12.53; O, 9.54. Found: C, 71.08; H, 6.98; N, 12.85; O, 9.22.

#### *N*-(3-(1*H*-Indol-2-yl)phenyl)acetamide (6)[20]

3-(1*H*-Indol-2-yl)aniline **1** (40 g, 192 mmol) was refluxed with glacial acetic acid (100 mL) for 3 h, the reaction mixture was concentrated to half its volume and water was added to give the acetylated product which was filtered and crystallized from ethanol. Green precipitate (yield 64%); m.p. 194–196°C; IR (KBr) $cm^{-1}$: 3404 (NH indole, $\underline{NH}$-C═O), 2923 (CH aliphatic), 1663 (C═O amidic); $^1$H-NMR (DMSO-$d_6$) (δ, ppm): 2.09 (s, 3H, $\underline{CH}_3$); 6.73 (s, 1H, H-3 indole); 6.97–6.99 (m, 1H, Ar-H); 7.11–7.21 (m, 1H, Ar-H); 7.35–7.73 (m, 5H, Ar-H); 8.01–8.05 (m, 1H, Ar-H); 10.00 (s, 1H, N$\underline{H}$CO, $D_2O$ exchangeable); 11.48 (s, 1H, NH indole, $D_2O$ exchangeable); EIMS, *m/z*: 250 ($M^+$); Anal. calcd. for $C_{16}H_{14}N_2O$ (250.11): C, 76.78; H, 5.64; N, 11.19; O: 6.39. Found: C, 76.28; H, 5.33; N, 10.89; O, 6.77.

#### *N*-(3-(3-Formyl-1*H*-indol-2-yl)phenyl)acetamide (7)

Phosphorous oxychloride (12 mL, 80 mmol) was dropwisely added to dimethylformamide (18 mL, 240 mmol) while cooling in an ice bath for 1 h. A solution of *N*-(3-(1*H*-indol-2-yl)phenyl)acetamide **6** (10 g, 40 mmol) in dimethylformamide (20 mL) was portionwisely added to the formylating mixture at 0–10°C and the temperature was raised and kept at 35°C for 1.5 h. The mixture was then poured onto ice/cold water and neutralized with sodium hydroxide solution to give a yellow precipitate which was collected by vacuum filtration and purified by column chromatography using ethyl acetate/petroleum ether (60:80)/chloroform in a ratio of 3:2:1. Yield 35%; m.p. 250–252°C; IR (KBr) $cm^{-1}$: 3435, 3262 (NH indole, NH-C═O), 2929 (CH aliphatic), 1676 (C═O aldehydic), 1640 (C═O amidic); $^1$H-NMR (DMSO-$d_6$) (δ, ppm): 2.09 (s, 3H, $\underline{CH}_3$); 7.21–7.32 (m, 2H, Ar-H); 7.39–7.41 (m, 1H, Ar-H); 7.45–7.55 (m, 2H, Ar-H); 7.66 (d, 1H, Ar-H, *J* = 7.8 Hz); 7.94–7.96 (m, 1H, Ar-H); 8.20 (d, 1H, Ar-H, *J* = 9 Hz); 10.00 (s, 1H, C$\underline{H}$O); 10.16 (s, 1H, NHC═O, $D_2O$ exchangeable); 12.38 (s, 1H, NH indole, $D_2O$ exchangeable); $^{13}$C-NMR (DMSO-$d_6$) (δ, ppm): 24.5, 112.5, 114.0, 120.6, 120.7, 121.5, 122.9, 124.2, 124.6, 126.1, 129.9, 130.5, 136.3, 140.2, 149.4, 169.1, 186.0. EIMS, *m/z*: 278 ($M^+$); Anal. calcd. for $C_{17}H_{14}N_2O_2$ (278.11): C, 73.37; H, 5.07; N, 10.07; O, 11.50. Found: C, 73.28; H, 5.63; N, 10.89; O, 11.77.

### 4.1.6 | General procedure for the synthesis of 2-((2-(3-acetamidophenyl)-1*H*-indol-3-yl)methylene)-hydrazinecarboxamide (8a) and *N*-(3-(3-((2-isonicotinyl/2-chlorophenylhydrazono)methyl)-1*H*-indol-2-yl)phenyl)acetamide (8b,c)

*N*-(3-(3-Formyl-1*H*-indol-2-yl)phenyl)acetamide **7** (0.5 g, 1.8 mmol) and semicarbazide hydrochloride or isonicotinic acid hydrazide or *o*-chlorophenylhydrazine hydrochloride, respectively (1.9 mmol), were refluxed in absolute ethanol (20 mL) in the presence of 2–3 drops of glacial acetic acid for 2 h. The solution was concentrated to half its volume and diluted with water. A precipitate was formed, filtered and crystallized from ethanol.

#### 2-((2-(3-Acetamidophenyl)-1*H*-indol-3-yl)methylene)hydrazine carboxamide (8a)

Yellowish brown crystals (yield 37%); m.p. 130–132°C; IR (KBr) $cm^{-1}$: 3435, 3318, & 3142 (NH indole, NH-C═O, N-NH), 1676 (C═O amidic), 1585 (C═N); $^1$H-NMR (DMSO-$d_6$) (δ, ppm): 2.10 (s, 3H, $\underline{CH}_3$); 7.14–7.99 (m, 8H, Ar-H); 8.19 (s, 1H, C$\underline{H}$═N); 9.45 (s, 2H, N$\underline{H}_2$, $D_2O$ exchangeable); 9.86 (s, 1H, N$\underline{H}$C═O, $D_2O$ exchangeable); 10.34 (s,1H, N-N$\underline{H}$, $D_2O$ exchangeable); 11.78 (s,1H, NH indole, $D_2O$ exchangeable); $^{13}$C-NMR (DMSO-$d_6$) (δ, ppm): 24.5, 108.3, 112.0, 119.6, 120.2, 121.1, 122.7, 124.1, 125.6, 125.7, 129.7, 130.1, 132.1, 136.9, 138.7, 140.2, 158.3, 169.2; EIMS, *m/z*: 335 ($M^+$); Anal. calcd. for $C_{18}H_{17}N_5O_2$ (335.14): C, 64.47; H, 5.11; N, 20.88; O, 9.54. Found: C, 64.08; H, 5.62; N, 20.67; O, 9.77.

#### *N*-(3-(3-((2-Isonicotinoylhydrazono)methyl)-1*H*-indol-2-yl)-phenyl)acetamide (8b)

Green crystals (yield 35%); m.p. 257–259°C; IR (KBr) $cm^{-1}$: 3392, 3260 (NH indole, NH-C═O), 1665 (C═O amidic), 1597 (C═N); $^1$H-NMR (DMSO-$d_6$) (δ, ppm): 2.09 (s, 3H, $CH_3$); 7.20–7.83 (m, 8H, Ar-H); 8.44–8.71 (m, 4H, Ar-H); 8.76 (s, 1H, C$\underline{H}$═N); 10.16 (s, 1H, N$\underline{H}$C═O, $D_2O$ exchangeable); 11.75 (s, 1H, N-NH, $D_2O$ exchangeable); 11.91 (s, 1H, NH indole, $D_2O$ exchangeable); EIMS *m/z* (%): 397 ($M^+$), 7.7%; Anal. calcd. for $C_{23}H_{19}N_5O_2$ (397.15): C,69.51; H, 4.82; N, 17.62; O, 8.05. Found C, 69.28; H, 5.02; N, 17.89, O, 8.77.

#### *N*-(3-(3-((2-(2-Chlorophenyl)hydrazono)methyl)-1*H*-indol-2-yl)-phenyl)acetamide (8c)

Light brown crystals (yield 30%); m.p. 137–139°C; IR (KBr) $cm^{-1}$: 3396, 3250 (NH indole, NH-C═O, N-NH), 2919 (CH aliphatic), 1667 (C═O amidic), 1596 (C═N); $^1$H-NMR (DMSO-$d_6$) (δ, ppm): 2.09 (s, 3H, $\underline{CH}_3$); 6.74–8.35 (m, 12H, Ar-H); 8.61 (s, 1H, C$\underline{H}$═N); 9.55 (s, 1H, N-N$\underline{H}$, $D_2O$ exchangeable); 10.16 (s, 1H, N$\underline{H}$C═O, $D_2O$ exchangeable); 11.66 (s, 1H, NH indole, $D_2O$ exchangeable); EIMS, *m/z*: 404 ($M^+$+2), 403 ($M^+$+1), 402 ($M^+$); Anal. calcd. for $C_{23}H_{19}ClN_4O$ (402.12): C, 68.57; H, 4.75; Cl, 8.80; N, 13.91; O, 3.97. Found: C, 69.08; H, 4.02; Cl, 8.20; N, 13.67; O, 3.57.

### 4.1.7 | General procedure for the synthesis of (2-(3-acetamidophenyl)-1*H*-indol-3-yl)methylene derivatives (9a,b)

*N*-(3-(3-Formyl-1*H*-indol-2-yl)phenyl)acetamide **7** (0.5 g, 1.8 mmol) and the appropriate active methylene derivative (1.8 mmol) were refluxed in absolute ethanol (15 mL) in the presence of few drops of triethylamine for 3h. The reaction mixture was concentrated to half its volume and diluted with cold water where a precipitate was formed, filtered, and crystallized from ethanol.

**N-(3-(3-(2,2-Dicyanovinyl)-1*H*-indol-2-yl)phenyl)acetamide (9a)**

Yellow crystals (yield 49%); m.p. 160–162°C; IR (KBr) $cm^{-1}$: 3250 (NH), 2919 (CH aliphatic), 2217 (CN), 1564 (C═C). $^1$H-NMR (DMSO-$d_6$) ($\delta$, ppm): 2.10 (s, 3H, $\underline{CH_3}$); 7.02–8.08 (m, 8H, Ar-H); 8.15 (s, 1H, C$\underline{H}$═C); 10.23 (s, 1H, N$\underline{H}$C═O, $D_2O$ exchangeable); 13.08 (s, 1H, NH indole, $D_2O$ exchangeable). EIMS, *m/z*: 326 ($M^+$); Anal. calcd. for $C_{20}H_{14}N_4O$ (326.12): C, 73.61; H, 4.32; N, 17.17; O, 4.90. Found: C, 73.18; H, 4.21; N, 17.45; O, 5.22.

**Ethyl 3-(2-(3-acetamidophenyl)-1*H*-indol-3-yl)-2-cyanoacrylate (9b)**

Yellow crystals (yield 42.5%); m.p. 149–151°C; IR (KBr) $cm^{-1}$: 3262 (NH), 2921 (CH aliphatic), 2214 (CN), 1683 (C═O ester), 1575 (C═C); $^1$H-NMR (DMSO-$d_6$) ($\delta$, ppm): 1.24–1.29 (t, 3H, $CH_2$-C$\underline{H_3}$); 2.09 (s, 3H, $CH_3$); 4.22–4.29 (q, 2H, C$\underline{H_2}$-$CH_3$); 7.12–7.29 (m, 3H, Ar-H); 7.44–7.57 (m, 2H, Ar-H); 7.79 (d, 1H, Ar-H, *J* = 7.5 Hz); 7.85–7.90 (m, 2H, Ar-H, C$\underline{H}$═C); 8.18 (d, 1H, Ar-H, *J* = 6 Hz); 10.20 (s, 1H, N$\underline{H}$-C═O, $D_2O$ exchangeable); 12.70 (s, 1H, NH indole, $D_2O$ exchangeable); EIMS, *m/z*: 373 ($M^+$); Anal. calcd. for $C_{22}H_{19}N_3O_3$ (373.14): C, 70.76; H, 5.13; N, 11.25; O, 12.85. Found: C, 71.01; H, 4.64; N, 11.31; O, 12.36.

### 4.1.8 | Synthesis of *N*-chloroacetyl sulfonamide derivatives (10a–e)[23,24]

Compounds **10a–e** were prepared according to the procedure cited in literature. Yield: 60–80%; m.p. are 216–218, 146–148, 235–237, 192–194, 228–230°C, respectively.

### 4.1.9 | Synthesis of 4-((4-oxo-4,5-dihydrothiazol-2-yl)-amino)benzene sulfonamide derivatives (11a–e)[16]

Compounds **11a–e** were synthesized according to the reported procedure. Yield: 73–90%; m.p. are 244–246, 259–261, 297°C decomposed, 240–242, >300°C, respectively.

### 4.1.10 | Synthesis of 1*H*-indole-3-carbaldehyde (13)[25–29]

It was synthesized from 1*H*-indole **12** according to the reported procedure. Yield: 81%; m.p. 194°C (Lit., 194–196°C).[25–29]

### 4.1.11 | General procedure for the synthesis of 4-((5-((1*H*-indol-3-yl)methylene)-4-oxo-4,5-dihydrothiazol-2-yl)-amino)benzenesulfonamide derivatives (14a–e)

A mixture of indole-3-carbaldehyde **13** (1.45 g, 10 mmol), the appropriate thiazolidinone **11a–e** (10 mmol) and anhydrous sodium acetate (0.82 g, 10 mmol) in glacial acetic acid (15 mL) was refluxed for 5–18 h. The separated solid was filtered while hot, washed with hot water and crystallized from dimethylformamide/water, except compounds **14b**,**d** were crystallized from ethanol.

**4-((5-((1*H*-Indol-3-yl)methylene)-4-oxo-4,5-dihydrothiazol-2-yl)-amino)benzene sulfonamide (14a)[31]**

Green crystals (yield 60%); m.p. >300°C; reaction time 5 h; IR (KBr) $cm^{-1}$: 3396, 3310, 3240 (NH, $NH_2$), 3046 (CH aromatic), 1667 (C═O amidic), 1319 ($SO_2$ asymmetric), 1155 ($SO_2$ symmetric); $^1$H-NMR (DMSO-$d_6$) ($\delta$, ppm): 7.04–7.20 (m, 4H, Ar-H); 7.32 (s, 2H, N$\underline{H_2}$, $D_2O$ exchangeable); 7.49 (d, 1H, Ar-H, *J* = 8 Hz); 7.70 (s, 1H, N$\underline{H}$, $D_2O$ exchangeable); 7.83–7.86 (m, 4H, 3Ar-H, H-2 indole); 7.93 (s, 1H, methine H); 11.88 (s, 1H, NH indole, $D_2O$ exchangeable); $^{13}$C-NMR (DMSO-$d_6$) ($\delta$, ppm): 111.0, 112.9, 116.0, 118.7, 121.3, 122.1, 123.4, 127.3, 127.7, 128.4, 136.70, 140.1, 151.8, 152.8, 164.2, 172.7. EIMS, *m/z*: 398 ($M^+$); Anal. calcd. for $C_{18}H_{14}N_4O_3S_2$ (398.46): C, 54.26; H, 3.54; N, 14.06; O, 12.05; S, 16.09. Found: C, 54.01; H, 3.14; N, 14.31; O, 12.66; S, 16.56.

**4-((5-((1*H*-Indol-3-yl)methylene)-4-oxo-4,5-dihydrothiazol-2-yl)-amino)-*N*-(5-methylisoxazol-3-yl)benzenesulfonamide (14b)**

Brown crystals (yield 50%); m.p. 268–270°C; reaction time 18 h; IR (KBr) $cm^{-1}$: 3332 (NH), 3062 (CH aromatic), 2927 (CH aliphatic), 1654 (C═O amidic), 1222 ($SO_2$ asymmetric), 1161 ($SO_2$ symmetric); $^1$H-NMR (DMSO-$d_6$) ($\delta$, ppm): 2.31 (s, 3H, $\underline{CH_3}$); 6.18 (s, 1H, C$\underline{H}$ isoxazole); 7.16–7.26 (m, 4H, Ar-H); 7.49 (d, 1H, Ar-H, *J* = 7.9 Hz); 7.66 (s, 1H, NH, $D_2O$ exchangeable); 7.87–7.96 (m, 5H; 3Ar-Hs, methine H, & H-2 indole); 11.45 (s, 1H, NH, $D_2O$ exchangeable); 11.94 (s, 1H, NH indole, $D_2O$ exchangeable); Anal. calcd. for $C_{22}H_{17}N_5O_4S_2$ (479.53): C, 55.10; H, 3.57; N, 14.60; O, 13.35; S, 13.37. Found: C, 55.38; H, 3.38; N, 14.85; O, 13.11; S, 13.66.

**4-((5-((1*H*-Indol-3-yl)methylene)-4-oxo-4,5-dihydrothiazol-2-yl)-amino)-*N*-(pyrimidin-2-yl)benzenesulfonamide (14c)**

Green crystals (yield 40%); m.p. >300°C; reaction time 18 h; IR (KBr) $cm^{-1}$: 3327, 3250 (NH), 3064 (CH aromatic), 1682 (C═O amidic), 1291 ($SO_2$ asymmetric), 1152 ($SO_2$ symmetric); $^1$H-NMR (DMSO-$d_6$) ($\delta$, ppm): 7.02–7.03 (m, 1H, Ar-H); 7.14–7.25 (m, 4H, Ar-H); 7.50 (d, 1H, Ar-H, *J* = 7.8 Hz); 7.64 (s, 1H, NH, $D_2O$ exchangeable); 7.85 (d, 1H, Ar-H, *J* = 7.5 Hz); 7.96–8.03 (m, 5H, 3Ar-H, H-2 indole & $SO_2$N$\underline{H}$); 8.50–8.52 (m, 2H, Ar-H & methine H); 11.97 (s, 1H, NH indole, $D_2O$ exchangeable). EIMS, *m/z*: 476 ($M^+$); Anal. calcd. for $C_{22}H_{16}N_6O_3S_2$ (476.53): C, 55.45; H, 3.38; N, 17.64; O, 10.07; S, 13.46. Found: C, 55.38; H, 3.78; N, 17.35; O, 10.51; S, 13.66.

**4-((5-((1*H*-Indol-3-yl)methylene)-4-oxo-4,5-dihydrothiazol-2-yl)-amino)-*N*-(pyridin-2-yl)benzenesulfonamide (14d)**

Green crystals (yield 45%); m.p. >300°C; reaction time 10 h; IR (KBr) $cm^{-1}$: 3389 (NH), 1630 (C═O amidic), 1292 ($SO_2$ assymetric), 1133 ($SO_2$ symetric); $^1$H-NMR (DMSO-$d_6$) (δ, ppm): 6.87–6.91 (m, 1H, Ar-H); 7.15–7.40 (m, 4H, Ar-H); 7.49 (d, 1H, Ar-H, *J* = 7.5 Hz); 7.63 (s, 1H, NH, $D_2O$ exchangeable); 7.74–8.04 (m, 9H; 6 Ar-Hs, H-2 indole, $SO_2$N<u>H</u> & methine H); 11.97 (s, 1H, NH indole, $D_2O$ exchangeable). EIMS, *m/z*: 475 ($M^+$); Anal. calcd. for $C_{23}H_{17}N_5O_3S_2$ (475.54): C, 58.09; H, 3.60; N, 14.73; O, 10.09; S, 13.49. Found: C, 58.38; H, 3.78; N, 14.35; O, 9.88; S, 13.66.

**4-((5-((1*H*-Indol-3-yl)methylene)-4-oxo-4,5-dihydrothiazol-2-yl)-amino)-*N*-(thiazol-2-yl)benzenesulfonamide (14e)**

Yellow crystals (yield 54%); m.p. 253–255°C; reaction time 21 h; IR (KBr) $cm^{-1}$: 3429, 3263 (NH), 1645 (C═O amidic), 1222 ($SO_2$ asymmetric), 1138 ($SO_2$ symmetric); $^1$H-NMR (DMSO-$d_6$) (δ, ppm): 6.84 (d, 1H, CH-5 thiazole, *J* = 4.5 Hz); 7.17–7.23 (m, 4H, Ar-H); 7.27 (d, 1H, CH-4 thiazole, *J* = 4.5 Hz); 7.49 (d, 1H, Ar-H, *J* = 7.7 Hz); 7.66 (s, 1H, NH, $D_2O$ exchangeable); 7.81–7.94 (m, 5H; 3Ar-H, H-2 indole & methine H); 11.90 (s, 1H, $SO_2$N<u>H</u>, $D_2O$ exchangeable); 12.25 (s, 1H, NH indole, $D_2O$ exchangeable); Anal. calcd. for $C_{21}H_{15}N_5O_3S_3$ (481.57): C, 52.38; H, 3.14 N, 14.54; O, 9.97; S, 19.98. Found: C, 52.48; H, 3.66; N, 14.35; O, 10.22; S, 19.66.

### 4.1.12 | Synthesis of *N*-benzoyl/*N*-(4-chlorobenzoyl)-glycine (15a,b)

Compounds **15a**,**b** were synthesized according to the reported procedure.[32,33] Yield: 90–95%; m.p. are 187–189C, 144–146°C, respectively.

### 4.1.13 | General procedure for the synthesis of (*Z*)-4-((1-acetyl-1*H*-indol-3-yl)methylene)-2-phenyl/4-chlorophenyl)oxazol-5(4*H*)-one (16a,b)

A mixture of indole-3-carbaldehyde **13** (1.45 g, 10 mmol), the appropriate *N*-benzoyl glycine/(hippuric acid) derivative **15a**,**b** (12 mmol) and fused sodium acetate (0.5 g, 6 mmol) in acetic anhydride (20 mL) was heated in a boiling water bath for 4 h. The mixture was cooled and ethanol was slowly added and allowed to stand overnight at 8°C (in refrigerator). A crystalline product was formed, filtered, washed with hot water and crystallized from petroleum ether (40:60).

**(*Z*)-4-((1-Acetyl-1*H*-indol-3-yl)methylene)-2-phenyloxazol-5(4*H*)-one (16a)[32,34]**

Yield: 46%; m.p. 203–205°C as reported in the literature.[34]

**(*Z*)-4-((1-Acetyl-1*H*-indol-3-yl)methylene)-2-(4-chlorophenyl)-oxazol-5(4*H*)-one (16b)**

Yellow crystals (yield 35%); m.p. 142–144°C; IR (KBr) $cm^{-1}$: 2928 (CH aliphatic), 1800 (O-C═O oxazolone), 1685 (C═O amidic), 1591 (C═C); $^1$H-NMR (DMSO-$d_6$) (δ, ppm): 2.77 (s, 3H, <u>$CH_3$</u>); 7.41–7.48 (m, 1H, Ar-H); 7.53 (d, 2H, Ar-H, *J* = 8.5 Hz); 7.70–7.75 (m, 1H, Ar-H); 7.93 (d, 2H, Ar-H, *J* = 8.5 Hz); 8.15–8.19 (m, 1H, Ar-H); 8.36–8.44 (m, 1H, Ar-H); 8.89 (s, 1H, methine H); 10.10 (s, 1H, H-2 indole; Anal. calcd. for $C_{20}H_{13}ClN_2O_3$ (364.06): C, 65.85; H, 3.59; N, 7.68; O, 13.16; Cl, 9.72. Found: C, 65.55; H, 3.79; N, 7.48; O, 13.66; Cl, 9.92.

### 4.1.14 | General procedure for the synthesis of (*Z*)-4-(4-((1-acetyl/1*H*-indol-3-yl)methylene)-5-oxo-2-phenyl/4-chlorophenyl-4,5-dihydro-1*H*-imidazol-1-yl)-benzene sulfonamide/*N*-substituted benzenesulfonamide (17a–d and 18a–c)

A mixture of the oxazolone derivative **16a**,**b** (10 mmol), the appropriate sulfonamide (10 mmol), and anhydrous sodium acetate (0.5 g, 6 mmol) in glacial acetic acid (20 mL) was heated in a boiling water bath for 1–30 h. Compounds **17a–d** were precipitated on hot, filtered, washed with hot water, and crystallized from dimethylformamide/water. Compounds **18a–c** were precipitated after pouring onto ice/cold water, filtered, washed with hot water, and purified with column chromatography using ethyl acetate/petroleum ether/chloroform 3:2:1.

**(*Z*)-4-(4-((1-Acetyl-1*H*-indol-3-yl)methylene)-5-oxo-2-phenyl-4,5-dihydro-1*H*-imidazol-1-yl)-*N*-(pyridin-2-yl)-benzenesulfonamide (17a)**

Yellow crystals (yield 30%); m.p. 278–280°C; reaction time 2 h; IR (KBr) $cm^{-1}$: 3429 (NH), 2925 (CH aliphatic); 1705 (C═O imidazolone), 1631 (C═O amidic); 1375 ($SO_2$ asymmetric), 1134 ($SO_2$ symmetric); $^1$H-NMR (DMSO-$d_6$) (δ, ppm): 2.77 (s, 3H, $CH_3$); 7.14–7.22 (m, 2H, Ar-H); 7.38–7.49 (m, 3H, Ar-H); 7.50–8.07 (m, 10H, 9Ar-H & C<u>H</u> methine); 8.34 (d, 1H, Ar-H, *J* = 8 Hz); 8.39 (d, 1H, Ar-H, *J* = 8 Hz); 8.49 (d, 1H, Ar-H, *J* = 8 Hz); 8.90 (s, 1H, H-2 indole); 10.58 (s, 1H, $SO_2$N<u>H</u>, $D_2O$ exchangeable); $^{13}$C-NMR (DMSO-$d_6$) (δ, ppm): 24.2, 115.1, 116.4, 116.5, 116.7, 119.8, 119.9, 120.4, 121.2, 124.2, 124.7, 125.9, 126.2, 127.7, 128.0, 128.4, 128.5, 128.9, 129.3, 129.7, 131.25, 131.4, 133.7, 135.0, 135.8, 137.5, 143.3, 159.1, 164.8, 169.0, 170.2. EIMS, *m/z*: 561 ($M^+$); Anal. calcd. for $C_{31}H_{23}N_5O_4S$ (561.61): C, 66.30; H, 4.13; N, 12.47; O, 11.40; S, 5.71. Found: C, 66.56; H, 4.18; N, 12.18; O, 11.99; S, 5.32.

**(*Z*)-4-(4-((1-Acetyl-1*H*-indol-3-yl)methylene)-5-oxo-2-phenyl-4,5-dihydro-1*H*-imidazol-1-yl)-*N*-(thiazol-2-yl)-benzenesulfonamide (17b)**

Yellow crystals (yield 40%); m.p. >300°C; reaction time 1h; IR (KBr) $cm^{-1}$: 3430 (NH), 2894 (CH aliphatic); 1705 (C═O imidazolone), 1631 (C═O amidic); 1376 ($SO_2$ asymmetric), 1146 ($SO_2$ symmetric); $^1$H-NMR (DMSO-$d_6$) (δ, ppm): 2.77 (s, 3H, C<u>$H_3$</u>); 6.88 (d, 1H, CH-5 thiazole, *J* = 4.5 Hz); 7.29 (d, 1H, CH-4 thiazole, *J* = 4.5 Hz); 7.42–7.46 (m, 5H, Ar-H); 7.52–7.56 (m, 4H, Ar-H); 7.58 (s, 1H, methine H); 7.88 (d, 2H, Ar-H, *J* = 8.3 Hz); 8.39 (d, 1H, Ar-H, *J* = 7.7 Hz); 8.49 (d, 1H, Ar-H, *J* = 7.2 Hz); 8.90 (s, 1H, H-2 indole); 12.84 (s, 1H, $SO_2$N<u>H</u>, $D_2O$ exchangeable); $^{13}$C-NMR (DMSO-$d_6$) (δ, ppm): 24.4, 109.1, 116.5, 116.8, 120.4, 121.2, 124.5, 125.2, 125.8, 126.2, 127.4, 128.6,

129.1, 129.4, 132.1, 133.7, 135.8, 137.7, 138.0, 141.7, 142.4, 159.0, 169.0, 169.5, 170.2; Anal. calcd. for $C_{29}H_{21}N_5O_4S_2$ (567.64): C, 61.36; H, 3.73; N, 12.34; O, 11.27; S, 11.30. Found: C, 61.88; H, 3.38; N, 12.85; O, 11.11; S, 11.66.

**(*Z*)-4-(4-((1-Acetyl-1*H*-indol-3-yl)methylene)-2-(4-chlorophenyl)-5-oxo-4,5-dihydro-1*H*-imidazol-1-yl)-*N*-(pyridin-2-yl)benzenesulfonamide (17c)**

Yellow crystals (yield 50%); m.p. 258–260°C; reaction time 2 h; IR (KBr) $cm^{-1}$: 3429 (NH), 2920 (CH aliphatic); 1714 (C═O imidazolone), 1634 (C═O amidic); 1379 ($SO_2$ asymmetric), 1141 ($SO_2$ symmetric); $^1$H-NMR (DMSO-$d_6$) ($\delta$, ppm): 2.78 (s, 3H, $CH_3$); 6.88–6.89 (m, 1H, Ar-H); 7.19–7.21 (m, 1H, Ar-H); 7.42–7.51 (m, 9H, Ar-H); 7.61 (s, 1H, methine H); 7.76–7.78 (m, 1H, Ar-H); 7.95 (d, 2H, Ar-H, $J$ = 7.8 Hz); 8.39 (d, 1H, Ar-H, $J$ = 8 Hz); 8.50 (d, 1H, Ar-H, $J$ = 7 Hz); 8.91 (s, 1H, H-2 indole); 12.20 (s, 1H, $SO_2NH$, $D_2O$ exchangeable); Anal. calcd. for $C_{31}H_{22}ClN_5O_4S$ (596.06): C, 62.47; H, 3.72; N, 11.75; O, 10.74; S, 5.38, Cl, 5.95. Found: C, 62.38; H, 3.98; N, 11.35; O, 10.88; S, 5.66; Cl, 5.68.

**(*Z*)-4-(4-((1-Acetyl-1*H*-indol-3-yl)methylene)-2-(4-chlorophenyl)-5-oxo-4,5-dihydro-1*H*-imidazol-1-yl)-*N*-(thiazol-2-yl)benzenesulfonamide (17d)**

Yellow crystals (yield 60%); m.p. 280–282°C; reaction time 2 h; IR (KBr) $cm^{-1}$: 3430 (NH), 2913 (CH aliphatic); 1715 (C═O imidazolone), 1636 (C═O amidic); 1376 ($SO_2$ asymmetric), 1148 ($SO_2$ symmetric); $^1$H-NMR (DMSO-$d_6$) ($\delta$, ppm): 2.78 (s, 3H, $CH_3$); 6.87 (d, 1H, CH-5 thiazole, $J$ = 4.5 Hz); 7.30 (d, 1H, CH-4 thiazole, $J$ = 4.5 Hz); 7.40–7.47 (m, 5H, Ar-H); 7.52–7.58 (m, 4H, Ar-H); 7.62 (s, 1H, methine H); 7.90 (d, 2H, Ar-H, $J$ = 8.3 Hz); 8.40 (d, 1H, Ar-H, $J$ = 7.6 Hz); 8.50 (d, 1H, Ar-H, $J$ = 7.3 Hz); 8.91 (s, 1H, H-2 indole); 12.83 (s, 1H, $SO_2NH$); $^{13}$C-NMR (DMSO-$d_6$) ($\delta$, ppm): 24.4, 116.4, 116.6, 120.8, 121.2, 124.7, 126.2, 127.7, 128.0, 128.5, 128.9, 129.1, 131.1, 133.89, 135.8, 136.8, 137.3, 137.6, 142.6, 149.3, 154.2, 158.1, 168.8, 170.2. EIMS, *m/z*: 601 ($M^+$); Anal. calcd. for $C_{29}H_{20}ClN_5O_4S_2$ (601.06): C, 57.85; H, 3.35; N, 11.63; O, 10.63; S, 10.65; Cl, 5.89. Found: C, 57.48; H, 3.66; N, 11.35; O, 10.22; S, 10.36; Cl, 6.23.

**(*Z*)-4-(4-((1*H*-Indol-3-yl)methylene)-5-oxo-2-phenyl-4,5-dihydro-1*H*-imidazol-1-yl)benzenesulfonamide (18a)**

Yellow crystals (yield 45%); m.p. 140–142°C; reaction time 28 h; IR (KBr) $cm^{-1}$: 3422 & 3264 ($NH_2$), 1707 (C═O imidazolone), 1373 ($SO_2$ asymmetric), 1160 ($SO_2$ symmetric); $^1$H-NMR (DMSO-$d_6$) ($\delta$, ppm): 7.23–7.28 (m, 3H, Ar-H); 7.40–7.56 (m, 8H, 6 Ar-H & $NH_2$); 7.67 (s, 1H, methine H); 7.89 (d, 3H, Ar-H, $J$ = 8 Hz); 8.40 (d, 1H, Ar-H, $J$ = 8 Hz); 8.61 (s, 1H, H-2 indole); 12.17 (s, 1H, NH indole, $D_2O$ exchangeable); Anal. calcd. for $C_{24}H_{18}N_4O_3S$ (442.49): C, 65.14; H, 4.10; N, 12.66; O, 10.85; S, 7.25. Found: C, 65.01; H, 4.54; N, 12.31; O, 10.66; Cl, 7.56.

**(*Z*)-4-(4-((1*H*-Indol-3-yl)methylene)-5-oxo-2-phenyl-4,5-dihydro-1*H*-imidazol-1-yl)-*N*-(5-methylisoxazol-3-yl)-benzenesulfonamide (18b)**

Orange crystals (yield 35%); m.p. 120–122°C; reaction time 30 h; IR (KBr) $cm^{-1}$: 3404 (NH), 2922 (CH aliphatic), 1704 (C═O imidazolone), 1631 (C═O amidic), 1373 ($SO_2$ asymmetric), 1162 ($SO_2$ symmetric; $^1$H-NMR (DMSO-$d_6$) ($\delta$, ppm): 2.32 (s, 3H, $CH_3$); 6.16 (s, 1H, CH isoxazole); 7.22–7.26 (m, 3H, Ar-H); 7.375–7.52 (m, 5H, Ar-H); 7.67 (s, 1H, methine H); 7.91–8.08 (m, 2H, Ar-H); 8.10–8.15 (m, 1H, Ar-H); 8.41–8.45 (m, 1H, Ar-H); 8.61 (s, 1H, H-2 indole); 11.56 (s, 1H, $SO_2NH$, $D_2O$ exchangeable), 12.18 (s, 1H, NH indole, $D_2O$ exchangeable); Anal. calcd. for $C_{28}H_{21}N_5O_4S$ (523.56): C, 64.23; H, 4.04; N, 13.38; O, 12.22; S, 6.12. Found: C, 64.77; H, 4.13; N, 13.87; O, 11.88; Cl, 5.97.

**(*Z*)-4-(4-((1*H*-Indol-3-yl)methylene)-2-(4-chlorophenyl)-5-oxo-4,5-dihydro-1*H*-imidazol-1-yl)benzenesulfonamide (18c)**

Orange crystals (yield 60%); m.p. 158–160°C; reaction time 26 h; IR (KBr) $cm^{-1}$: 3423, 3264 (NH, $NH_2$), 1706 (C═O imidazolone); 1379 ($SO_2$ asymmetric), 1160 ($SO_2$ symmetric); $^1$H-NMR (DMSO-$d_6$) ($\delta$, ppm): 7.21–7.28 (m, 2H, Ar-H); 7.45–7.58 (m, 9H, 7Ar-H & $NH_2$); 7.69 (s, 1H, methine H); 7.90 (dd, 2H, Ar-H, $J$ = 4.2, 4.42 Hz); 8.40 (d, 1H, Ar-H, $J$ = 6.5 Hz); 8.61 (s, 1H, H-2 indole); 12.20 (s, 1H, NH indole, $D_2O$ exchangeable); Anal. calcd. for $C_{24}H_{17}ClN_4O_3S$ (476.93): C, 60.44; H, 3.59; N, 11.75; O, 10.06; S, 6.72, Cl, 7.43. Found: C, 60.38; H, 3.78; N, 11.35; O, 10.51; S, 6.66; Cl, 7.89.

## 4.2 | Molecular docking study

All the molecular modeling studies were carried out using Molecular Operating Environment (MOE, 10.2008) software. All minimizations were performed with MOE until an RMSD gradient of 0.05 kcal · $mol^{-1}$ $Å^{-1}$ with MMFF94x force field and the partial charges were automatically calculated. The X-ray crystallographic structure of VEGFR-2 co-crystallized with sorafenib as inhibitor (PDB ID: 4ASD) was downloaded from the Protein Data Bank.[45] The protein was prepared for docking study using Protonate 3D protocol in MOE with default options followed by water molecules removal. The co-crystalized ligand was used to define the active site for docking. Triangle Matcher placement method and London dG scoring function were used for docking. Docking setup was first validated by re-docking of the co-crystallized ligand (sorafenib) in the vicinity of the active site of the protein with energy score (S) = −15.19 kcal/mol and RMSD of 0.470 Å. The validated setup was then used in predicting the ligand receptor interactions at the active site for the newly synthesized compounds.

## 4.3 | Biological studies

### 4.3.1 | *In vitro* antiproliferative activity

The cytotoxicity assays for the synthesized compounds were performed against 60 cell line panel at the National Cancer Institute (NCI), Bethesda, Maryland, USA under the Developmental Therapeutic Program (DTP).[37] Compounds with drug-like mode of action, based on computer-aided design, are to be prioritized in the NCI screening service. Selection of the compounds for anticancer screening is based on the ability of the submitted compounds to add diversity to the NCI

small molecule compound libraries. The operation of this screening panel utilizes 60 different human tumor cell lines. The experimental for the single dose screen is reported as a mean graph at a single dose of 10 μM in detail (Supporting Information).

### 4.3.2 | *In vitro* determination of VEGFR-2 level for selected compounds in MCF-7 cell line

Ten compounds (**3b**, **5a**, **5b**, **6**, **8b**, **14a**, **14b**, **14d**, **14e**, and **18c**) have been selected for the study of inhibition of VEGFR-2 level in MCF-7 carcinoma cell line obtained from the American Type Culture Collection (Rockville, MD, USA). The level of human VEGFR-2 in samples was calculated (ng/mL) as triplicate determinations from the standard curve. Percent inhibition was calculated by the comparison of the tested compounds treated to control cancer cells. The obtained data were compared with sorafenib as a VEGFR-2 inhibitor. The experimental for this *in vitro* assay is given in detail in the Supporting Information.

### 4.3.3 | *In vitro* VEGFR-2 kinase assay

Seven compounds namely, **5a**, **5b**, **6**, **7**, **14b**, **18b**, and **18c** were evaluated for their *in vitro* inhibitory activity against human VEGFR-2 using ELISA (Enzyme Linked Immunosorbent Assay) kit according to manufacturer's instructions (Cell Signaling Technology, Inc., USA). The microtiter plate provided in this kit had been pre-coated with horseradish peroxidase (HRP) labeled secondary antibody (anti-rabbit IgG) specific to VEGFR-2. Standards and samples were added to the appropriate microtiter plate wells. Tetramethyl benzidine (TMB) substrate was added and incubated at room temperature and the stop solution was then added. The color change was measured colorimetrically at a wavelength of 450 ± 10 nm using a microtiter plate reader. Percent inhibition was calculated by the comparison of compounds treated to control incubations. The concentration of the test compound causing 50% inhibition ($IC_{50}$) was calculated from the concentration inhibition response curve and the data were compared with the lead compound sorafenib.

## ACKNOWLEDGMENTS

The authors thank the "National Research Centre (NRC)" for financially supporting the manuscript through the fund of the NRC project no. P100220. The authors are grateful to the National Cancer Institute (NCI), Developmental Therapeutic Program (DTP), US to perform the anticancer screening. Deep thanks are expressed to Dr. Wagdy M. Eldehna, Department of Pharmaceutical Chemistry, Faculty of Pharmacy, Egyptian Russian University, Badr City, Cairo, Egypt for providing sorafenib.

## CONFLICTS OF INTEREST

The authors have declared no conflict of interest.

## ORCID

*Iman A. Y. Ghannam* http://orcid.org/0000-0003-3176-0187

## REFERENCES

[1] C. Avendano, J. C. Menendez, *Medicinal Chemistry of Anticancer Drugs*, 1st ed., Elsevier Science, Barcelona **2008**. pp. 1–442.
[2] S. Di Martino, A. Raninone, A. Troise, M. Di Paolo, S. Pugliese, S. Zappavigna, A. Grimaldi, D. Valente, *WCRJ* **2015**, *2*, e533.
[3] S. Payne, D. Miles, *Scott-Brown's Otorhinolaryngology: Head and Neck Surgery* (Ed: M.J. Gleeson), CRC Press, London **2008**, Ch. 4.
[4] E. M. Bridges, A. L. Harris, *Biochem. Pharmacol.* **2011**, *81*, 1183.
[5] P. Saharinen, L. Eklund, K. Pulkki, P. Bono, K. Alitalo, *Trends Mol. Med.* **2011**, *17*, 347.
[6] N. Ferrara, H. P. Gerber, J. LeCouter, *Nat. Med.* **2003**, *9*, 669.
[7] S. Oudard, B. Beuselinck, J. Decoene, P. Albers, *Cancer Treat. Rev.* **2011**, *37*, 178.
[8] D. Xu, T. L. Wang, L. P. Sun, Q. D. You, *Mini-Rev. Med. Chem.* **2011**, *11*, 18.
[9] M. Pettersson, *Modern Drug Synthesis* (Eds: J. Li, D. Johnson), John Wiley & Sons, New York **2010**, Ch. 7.
[10] C. Gridelli, P. Maione, F. Del Gaizo, G. Colantuoni, C. Guerriero, C. Ferrara, D. Nicolella, D. Comunale, A. De Vita, A. Rossi, *Oncologist* **2007**, *12*, 191.
[11] P. Imming, C. Sinning, A. Meyer, *Nat. Rev. Drug Discov.* **2006**, *5*, 821.
[12] A. Temirak, Y. M. Shaker, F. A. Ragab, M. M. Ali, S. M. Soliman, J. Mortier, G. Wolber, H. I. Ali, H. I. El Diwani, *Arch. Pharm. (Weinheim)* **2014**, *347*, 291.
[13] Y. Li, C. Tan, C. Gao, C. Zhang, X. Luan, X. Chen, H. Liu, Y. Chen, Y. Jiang, *Bioorg. Med. Chem.* **2011**, *19*, 4529.
[14] S. S. El-Nakkady, M. M. Hanna, H. M. Roaiah, I. A. Y. Ghannam, *Eur. J. Med. Chem.* **2012**, *47*, 387.
[15] T. D. Bradshaw, S. Wrigley, D. F. Shi, R. J. Schultz, K. D. Paull, M. F. Stevens, *Br. J. Cancer* **1998**, *77*, 745.
[16] F. M. Awadallah, T. A. El-Waei, M. M. Hanna, S. E. Abbas, M. Ceruso, B. E. Oz, O. O. Guler, C. T. Supuran, *Eur. J. Med. Chem.* **2015**, *96*, 425.
[17] C. Karaaslan, H. Kadri, T. Coban, S. Suzen, A. D. Westwell, *Bioorg. Med. Chem. Lett.* **2013**, *23*, 2671.
[18] X. Yu, E. J. Park, T. P. Kondratyuk, J. M. Pezzuto, D. Sun, *Org. Biomol. Chem.* **2012**, *10*, 8835.
[19] A. K. Agrawal, V. K. Rastogi, S. S. Parmar, *J. Heterocyclic Chem.* **1978**, *15*, 677.
[20] X. Wang, D. V. Gribkov, D. Sames, *J. Org. Chem.* **2007**, *72*, 1476.
[21] T. Lemster, U. Pindur, G. Lenglet, S. Depauw, C. Dassi, M. H. David-Cordonnier, *Eur. J. Med. Chem.* **2009**, *44*, 3235.
[22] S. Suzen, P. Bozkaya, T. Coban, D. Nebiogu, *J. Enzyme Inhib. Med. Chem.* **2006**, *21*, 405.
[23] I. O. Donkor, Y. S. Abdel-Ghany, P. F. Kador, T. Mizoguchi, A. Bartoszko-Mailk, D. D. Miller, *Eur. J. Med. Chem.* **1998**, *33*, 15.
[24] J. Finkelstein, *J. Am. Chem. Soc.* **1944**, *66*, 407.
[25] C. I. Canche Chay, R. Gomez Cansino, C. I. Espitia Pinzon, R. O. Torres-Ochoa, R. Martinez, *Mar. Drugs* **2014**, *12*, 1757.
[26] R. Guillon, C. Loge, F. Pagniez, V. Ferchaud-Roucher, M. Duflos, C. Picot, P. Le Pape, *J. Enzyme Inhib. Med. Chem.* **2011**, *26*, 261.
[27] P. James, H. Snyder, *Org. Synth.* **1959**, *39*, 30.
[28] H. R. Snyder, S. Swaminathan, H. J. Sims, *J. Am. Chem. Soc.* **1952**, *74*, 5110.
[29] A. C. Shabica, E. E. Howe, J. B. Ziegler, M. Tishler, *J. Am. Chem. Soc.* **1946**, *68*, 1156.
[30] G. A. El-Hag Ali, A. Khalil, A. H. Ahmed, M. S. El-Gaby, *Acta Chim. Slov.* **2002**, *49*, 365.
[31] M. Ge, W. Mei, G. Weijuan, Z. Xiehe, L. Jia, L. Jingya, G. Lixin (Xi'an Jiaotong University; National Center for Drug Screening) CN 104059060. **2014**.

[32] K. M. Khan, U. R. Mughal, M. T. Khan, U. Zia, S. Perveen, M. I. Choudhary, *Bioorg. Med. Chem.* **2006**, *14*, 6027.
[33] B. Furniss, A. Hannaford, P. Smith, A. Tactchell, *Vogel's Textbook of Practical Organic Chemistry* (Ed: A. I. Vogel), Longman Scientific & Technical, Harlow **1989**, p. 1155.
[34] D. Donati, A. G. Aburbeh, B. Natalini, C. Marchioro, R. Pellicciari, *Tetrahedron* **1996**, *52*, 9901.
[35] M. McTigue, B. W. Murray, J. H. Chen, Y. L. Deng, J. Solowiej, R. S. Kania, *Proc. Natl. Acad. Sci. USA* **2012**, *109*, 18281.
[36] W. M. Eldehna, S. M. Abou-Seri, A. M. El Kerdawy, R. R. Ayyad, A. M. Hamdy, H. A. Ghabbour, M. M. Ali, D. A. Abou El Ella, *Eur. J. Med. Chem.* **2016**, *113*, 50.
[37] *National Cancer Institute – Developmental Therapeutics Program*, www.dtp.nci.nih.gov
[38] M. Boyd, K. Paull, *Cancer Drug Discovery and Development: Anticancer Drug Development Guide: Preclinical Screening, Clinical Trials and Approval* (Ed: B. A. Teicher), Humana Press, Totowa **2014**, Ch. 2.
[39] R. Shoemaker, *Nat. Rev. Cancer* **2006**, *6*, 813.
[40] M. Boyd, K. Paull, *Drug Dev. Res.* **1995**, *34*, 91.
[41] P. Skehan, R. Storeng, D. Scudiero, A. Monks, J. McMahon, D. Vistica, J. T. Warren, H. Bokesch, S. Kenney, M. R. Boyd, *J. Natl. Cancer Inst.* **1990**, *82*, 1107.
[42] M. C. Alley, D. A. Scudiero, A. Monks, M. L. Hursey, M. J. Czerwinski, D. L. Fine, B. J. Abbott, J. G. Mayo, R. H. Shoemaker, M. R. Boyd, *Cancer Res.* **1988**, *48*, 589.
[43] M. A. Abdullaziz, H. T. Abdel-Mohsen, A. M. El Kerdawy, F. A. F. Ragab, M. M. Ali, S. M. Abu-Bakr, A. S. Girgis, H. I. El Diwani, *Eur. J. Med. Chem.* **2017**, *136*, 315.
[44] S. Guo, L. S. Colbert, M. Fuller, Y. Zhang, R. R. Gonzalez-Perez, *Biochim. Biophys. Acta* **2010**, *1806*, 108.
[45] *RSCB Protein Data Bank*, http://www.rcsb.org/.

## SUPPORTING INFORMATION

Additional Supporting Information may be found online in the supporting information tab for this article.

**How to cite this article:** Roaiah HM, Ghannam IAY, Ali IH, et al. Design, synthesis, and molecular docking of novel indole scaffold-based VEGFR-2 inhibitors as targeted anticancer agents. *Arch Pharm Chem Life Sci.* 2018;1–17. https://doi.org/10.1002/ardp.201700299